TIME SERIES ANALYSES OF A GREAT BASIN GROUNDWATER-FED WETLAND COMPLEX, JUAB COUNTY, UTAH: CLIMATE EFFECTS ON GROUNDWATER-DEPENDENT WETLANDS

by Paul Inkenbrandt

REPORT OF INVESTIGATION 282
UTAH GEOLOGICAL SURVEY 2020
UTAH DEPARTMENT OF NATURAL RESOURCES

Blank pages are intentional for printing purposes.

TIME SERIES ANALYSES OF A GREAT BASIN GROUNDWATER-FED WETLAND COMPLEX, JUAB COUNTY, UTAH: CLIMATE EFFECTS ON GROUNDWATER-DEPENDENT WETLANDS

by Paul Inkenbrandt

Cover photo: *View of a part of the Leland Harris wetland complex, with the Confusion Range in the background.*

Suggested citation:

Inkenbrandt, P., 2020, Time series analyses of a Great Basin groundwater-fed wetland complex, Juab County, Utah—climate effects on groundwater-dependent wetlands: Utah Geological Survey Report of Investigation 282, 26 p., https://doi.org/10.34191/RI-282.

REPORT OF INVESTIGATION 282
UTAH GEOLOGICAL SURVEY
a division of
UTAH DEPARTMENT OF NATURAL RESOURCES
2020

STATE OF UTAH
Gary R. Herbert, Governor

DEPARTMENT OF NATURAL RESOURCES
Brian Steed, Executive Director

UTAH GEOLOGICAL SURVEY
R. William Keach II, Director

PUBLICATIONS
contact
Natural Resources Map & Bookstore
1594 W. North Temple
Salt Lake City, UT 84116
telephone: 801-537-3320
toll-free: 1-888-UTAH MAP
website: utahmapstore.com
email: geostore@utah.gov

UTAH GEOLOGICAL SURVEY
contact
1594 W. North Temple, Suite 3110
Salt Lake City, UT 84116
telephone: 801-537-3300
website: geology.utah.gov

CONTENTS

FIGURES

TABLES

TIME SERIES ANALYSES OF A GREAT BASIN GROUNDWATER-FED WETLAND COMPLEX, JUAB COUNTY, UTAH: CLIMATE EFFECTS ON GROUNDWATER-DEPENDENT WETLANDS

by Paul Inkenbrandt

ABSTRACT

This project assessed the effects of climate variability on wetland water levels using aquifer, wetland, and stream data collected from an existing monitoring network in Snake Valley, Utah and Nevada, specifically focusing on the Leland Harris wetland complex. This network includes 78 aquifer piezometers, 50 active wetland piezometers, and 9 surface flow gages in the Snake and Tule Valleys, where each station measures hourly water-level or flow values. Hydrologists at the Utah Geological Survey (UGS) are attempting to isolate all factors, including long-term climate signals, affecting water levels in the regional aquifer in Snake Valley. I contributed to these efforts by analyzing data from existing flow gages, wetland piezometers, and a recently installed weather station to establish more reliable evapotranspiration relationships for these arid wetlands. The objective for this project was to develop climate influence models for Snake Valley wetlands.

Open-source statistical software libraries available in the Python programming language were used to model and assess the time series data collected in the wetland complex and compare those data to climate data. There is a lagged correlation of water elevation at many of the piezometers and precipitation at nearby climate stations. The lags include one to two days, and potentially (correlation is weak) three years. Evapotranspiration can be estimated from changes in water level observed in the piezometers, and the monthly evapotranspiration at Leland Harris wetland complex varies between 0 inches in the winter to about 9 inches in the summer. Most of the climate and water level data show daily and yearly periodicities, which align to day-night and seasonal cycles, respectively. Lidar data were used to determine a relationship between area of wetland inundation and water level elevation, which in turn could be used as a metric for sensitive species. Models like Prophet and PASTAS can be used to better understand the influence of variables like evapotranspiration and precipitation, and Prophet seems well suited to predicting future water level elevations.

INTRODUCTION

Populations of sensitive species, like the Columbia spotted frog and the least chub, are dependent on the wetland habitats in western Utah. Quantifying the driving forces behind changes in these wetland habitats can make prediction of habitat degradation possible. The objective of this project was to develop groundwater level models for Snake Valley wetlands and to determine the driving forces in groundwater fluctuations in these wetland systems.

Study Area

Snake Valley is a Basin and Range fault-bounded valley within the Great Basin that straddles the Nevada-Utah state line. Snake Valley contains numerous isolated groundwater-fed wetlands along its axis, where groundwater discharge is dominant. The Utah Geological Survey (UGS) installed a network of groundwater monitoring wells and surface flow gages in Snake Valley in 2007-2008 in response to concerns of the Utah Legislature over Southern Nevada Water Authority (SNWA) proposals to develop groundwater in Spring Valley, Nevada, and the Nevada portion of Snake Valley. This network includes nested spring gradient wells in wetland complexes. The UGS added a wetland monitoring network in 2010, which consists of a series of piezometers ranging in depth from 5 to 25 feet. (1.5–7.6 m) Additional piezometers were added to the network in subsequent years.

The study area for this project is the Leland Harris wetland complex (henceforth referred to as Leland Harris) (figure 1). I chose this location because it has a complete monitoring record, with both spring gradient wells and piezometers. Leland Harris was also the focal point of earlier studies, which allows us to build on existing work. Leland Harris is exemplary of wetland systems in the Great Basin in that the dominant water input is groundwater and the dominant output is evaporation. Like other wetland systems in the Great Basin, the setting is the discharge area of an extensional basin-fill valley, which is adjacent to playa lakes and high-salinity water.

The valley-mountain topography of the Basin and Range Province, along with changes in climate in the last 20,000 years from generally wet to dry conditions, has led to a unique assemblage of aquatic organisms characterized by low species diversity and high endemism (Grover, 2019). These assemblages include the least chub (*Iotichthys phlegethontis*) and Columbia spotted frog (*Rana luteiventris*), which are both listed as sensitive species by the Utah Division of Wildlife Resources. Leland Harris is one of three wetland complexes in Snake Valley containing both species.

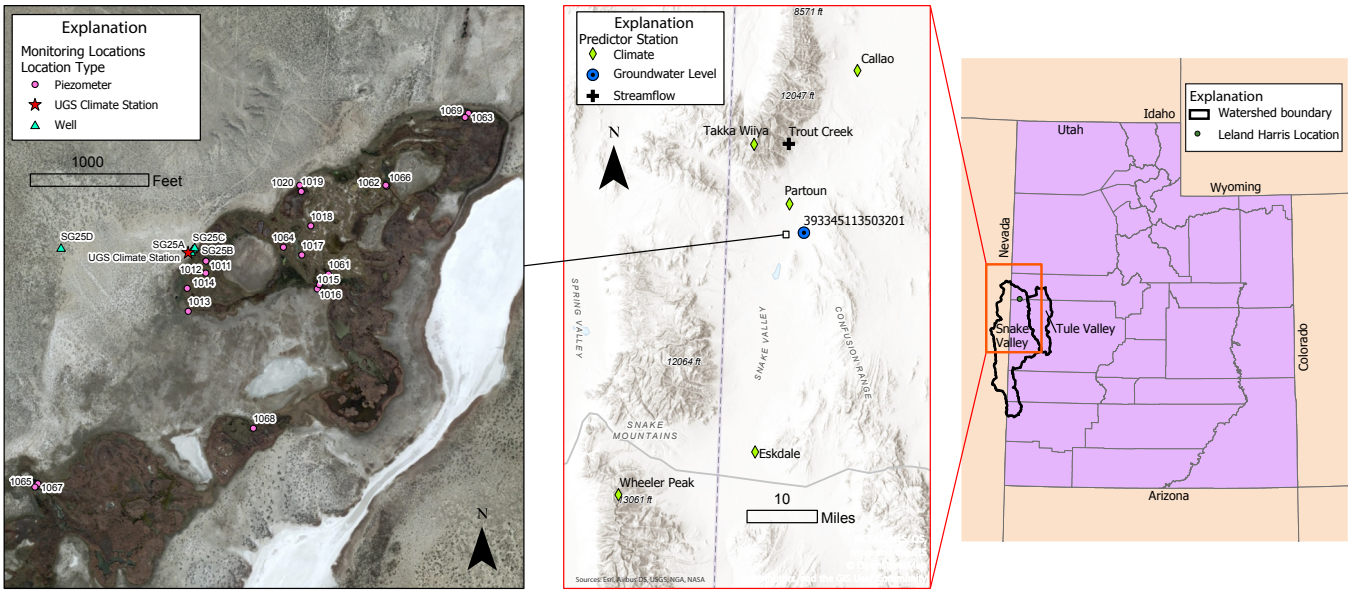

Figure 1. *Leland Harris wetland complex is in Snake Valley, a Basin and Range valley straddling the state line between Nevada and Utah. See tables 1 and 2 for descriptions of the monitoring locations and prediction stations, respectively.*

Previous Work

I conducted a literature review of similar studies to determine methods that are most applicable to this study. This section focuses on regional studies relevant to the study area, and method papers are cited in the Methods section of this report.

Grover (2016, 2019) conducted a hydrologic study of the Leland Harris wetland complex. He measured the bathymetry of the system using 3852 measurement locations, and revisited 47 of those locations monthly over several months to measure changes in surface water depth (Grover, 2016). Grover (2016) showed that about 80% of the temporal variation in surface water levels could be explained by variations in groundwater levels, and groundwater levels were negatively correlated with reference evapotranspiration (ET) rates provided by the Utah Climate Center, where extended ET rates reduced surface water levels. Ponds at Leland Harris are most responsive to changes in groundwater levels, followed by channels and springs, respectively. Grover (2016) defined multiple linear equations to describe the correlation between UGS Spring Gradient (SG) well 25D and the surface water depths at Leland Harris and summarized those equations with one that relates the average surface water level of all his measurement points to the depth to groundwater in SG25D:

$$y = 0.88x + 204.17 \quad (1)$$

where:

y = Average monthly surface water depth (cm)

x = Average monthly depth to groundwater (cm)

Because his measurement frequency was monthly at most, most of his equations aggregated at a monthly or larger scale. Grover (2019) went on to examine the relationship between least chub (*Iotichthys phlegethontis*) and Utah chub (*Gila atraria*) population counts with his surface water level measurements, determining that both species preferred deeper (>19 cm) locations in Leland Harris. Low surface water levels fragmented the Leland Harris chub habitat. Grover noted both species migrated to shallower areas for spawning during April, returning to deeper pools by June, and completely abandoning the shallowest areas by July. I have obtained all the relevant data from Mark Grover (Grover, 2016, 2019), whose research inspired the objectives of this report. Grover provided bathymetry and water depth data that will be useful in correlating with the wetland piezometer network.

Hurlow (2014) completed a major study of the groundwater flow system in Snake Valley. He summarized data from the UGS Snake Valley groundwater monitoring network, consisting of 70 monitoring wells. Like the wetland piezometers, groundwater levels in wells in the Snake Valley monitoring network are measured hourly. The network consists of agricultural monitoring wells, general potentiometric surface monitoring wells, and spring-gradient wells. Spring-gradient sites consist of nested piezometers near groundwater-dependent ecosystems, that measure the vertical hydraulic gradient feeding groundwater discharge (Hurlow, 2014). Hurlow (2014) found that evapotranspiration drove seasonal groundwater level fluctuations of 0.5 to 3 feet (0.15–0.9 m) in the area of Leland Harris.

Hurlow (2014) noted no significant year-to-year change in water levels at Leland Harris between 2008 and 2011. The spring gradient wells at Leland Harris generally show an up-

ward vertical hydraulic gradient of about 0.03 between 2008 and 2011. The U.S. Bureau of Land Management (Hurlow, 2014) estimated that the SNWA's proposed groundwater-development plan could cause up to 10 feet (3 m) of drawdown in the vicinity of Leland Harris within up to 200 years after full implementation of the project, including impacts to groundwater-dependent wetland ecosystems (Cooper and others, 2006, 2015; Patten and others, 2008). Other potentially affected systems include Gandy Warm Springs, Twin Springs and Foote Reservoir Spring, Kell Spring, Salt Marsh Lake spring complex, and Miller Spring. Hurlow (2014) categorized the Leland Harris system as a discharge area of intermediate flow systems in Snake Valley, like Salt Marsh Lake Springs in north-central Snake Valley and the Bishop Springs area (including Twin Springs and Foote Spring) in east-central Snake Valley. Intermediate-scale flow systems in Snake Valley likely recharge in the same areas as local flow systems, but may have groundwater with longer, deeper flow paths compared to local flow systems.

Ultimately, hydrologic models will be used to determine habitat suitability. Sáenz (2014) examined controlling factors on chub populations in Gandy Salt Marsh and Bishop Springs wetland complexes in Snake Valley. Least chub reproduction increases with increasing winter precipitation in Snake Valley wetlands (Sáenz, 2014). Persistence of both least chub and Utah chub is positively correlated to percent open water and average pool depth. The chubs use deep, open pools during the dry season (late summer) and expand out to the more expansive flooded areas during late winter and spring (Sáenz, 2014). As least chub and Utah chub accumulate in isolated spring pools during the dry season, the isolation can be lethal if patches dry out or dry to the point of limited water quality.

The U.S. Geological Survey (USGS) developed several large-scale models of the Great Basin and Snake Valley (Heilweil and Brooks, 2011; Masbruch and others, 2014; Masbruch, 2019). Groundwater models of Snake Valley predict partial to complete spring discharge depletion at several wetland locations under a variety of scenarios related to pending water right applications for groundwater withdrawal (Masbruch and others, 2014). Masbruch and others (2014) predicted a 35-cm reduction in shallow groundwater levels near Leland Harris if two nearby agricultural wells are approved and pumped.

METHODS

Methods for this project included (1) a rigorous initial analysis and plotting of the piezometer data to more closely visualize seasonality and outliers in the data, (2) seasonal decomposition and fast Fourier analysis on all the reprocessed hydrologic time series data to examine the periodicities in the data, (3) plotting water-year summaries of each piezometer, showing summary statistics for all available years over the course of a water year, and (4) generating heat maps of each well, which show flow intensity by month and year.

Collecting Groundwater Levels

To collect groundwater levels for Leland Harris, I used a combination of spring gradient wells and piezometers (table 1). For the purpose of this study, spring gradient (SG) wells refer to deeper, more permanent monitoring well installations, where the wells are located near each other but have screened intervals at different depths. Piezometers are shallower (typically less than 15 feet [7.6 m]), smaller diameter, less permanent monitoring wells installed closer to and within the wetland system. Spring-gradient well data are more representative of the more regional groundwater conditions, whereas piezometer data generally reflect the surface water conditions of the wetland.

There are 21 piezometers (table 1), four spring gradient wells (table 1), and one weather station installed at Leland Harris. Solinst non-vented pressure transducers were installed in most of the piezometers and wells, which measure water temperature and absolute pressure hourly on the hour. For this study, I focused on nine of the piezometers with the most complete and representative data records, as well as the spring gradient wells.

Manual depth-to-water measurements were recorded at each piezometer and well at least two times per year, along with well stickup, specific conductivity, and depth to water. Notes on vegetation cover and site photographs were also collected during the field visits. Lindsey Smith and Ben Erickson (UGS) recorded high precision elevation measurements of each of the piezometers in the Snake Valley wetland piezometer network. Improved elevation measurements from the wetland piezometers allow for a more meaningful application of the Grover data.

Python scripts were used to statistically summarize the water level data, computing the standardized median groundwater elevation. I first standardized water level data from each piezometer and then computed the median of all the standardized data for each hourly time step. Then the time steps were aggregated into yearly steps using the mean of the standardized medians. The same process was applied to the valley precipitation stations for comparison. I also computed general summary statistics of the water level and temperature data.

A separate analysis examined the hourly data for inflection points to better understand the general timing of major changes in groundwater levels. First, I aggregated the data from each well by averaging the water levels based on the day of the calendar year. Then the aggregated data from each well were smoothed using a 20-day moving average. I then conducted a changepoint analysis on the first derivative of the smoothed data and manually checked the automated changepoint analysis output, removing spurious changepoints that were inconsistent across the well data. Finally, the change-

points were grouped into seven major categories that represent major changes in slope in most of the hydrographs.

I also compiled groundwater level data from one USGS well (USGS Site 393345113503201) 2 miles (3.2 km) east of Leland Harris (table 2) (U.S. Geological Survey, 2019). The well is 200 feet (61 m) deep and has groundwater level measurements from August 1981 to March 2019. The sampling frequency ranges from monthly to yearly.

Compiling Predictor Data

I compiled climate data from five regional weather stations, including SNOTEL sites, and various climate indices (ENSO, MJO, circulation) (van Oldenborgh, 2020) to determine discernable or statistical correlation between the climate signals and the Leland Harris piezometer levels (table 2). I also compiled streamflow data from a USGS stream gage, Trout Creek (station 10172870; table 2). I established a new climate station

Table 1. *Piezometers and wells examined for this study.*

Site ID Number	Well Name	Used in Analyses	Elevation (ft amsl)	Latitude	Longitude	Install Date	Last Meas. Taken On	Stickup (ft)	Well Depth (ft)	Notes
1011		Yes	4783.196	39.5581	-113.8913	2009-10-15		1.02	4.1	
1012		Yes	4783.855	39.5584	-113.8913	2009-10-15		1.66	3.8	
1013		Yes	4783.225	39.5572	-113.8918	2009-10-15		0.8	4.1	
1014		Yes	4781.385	39.5577	-113.8919	2009-10-15		1.3	3.7	
1015		Yes	4781.988	39.5578	-113.8880	2009-11-11		1	4.1	
1016		Yes	4780.755	39.5579	-113.8879	2009-11-11		2.12	2.7	
1017		Yes	4778.59	39.5586	-113.8884	2009-11-11	2014-10-31	0.85	3.9	
1018			4780.571	39.5593	-113.8882	2009-11-11		1.15	4.2	
1019		Yes	4780.581	39.5601	-113.8885	2009-11-11		1.2	3.9	
1020		Yes	4781.933	39.5602	-113.8886	2009-11-11		0.8	4.2	
1061			4780.464	39.5582	-113.8876	2012-08-09		1	3.5	No transducer
1062			4780.438	39.5603	-113.8860	2012-08-09	2014-10-31	0.46	4.1	
1063			4781.214	39.5619	-113.8837	2012-08-09		0.75	4.4	
1064			4779.798	39.5588	-113.8890	2012-08-09	2014-10-31	0.5	3.6	
1065			4779.941	39.5531	-113.8961	2012-08-09		1.86	3.2	Open water around casing
1066			4780.537	39.5603	-113.8860	2012-08-09	2014-10-31	0.81	3.8	
1067			4780.371	39.5530	-113.8962	2012-08-09		0.16	4.6	
1068			4779.839	39.5545	-113.8897	2014-10-31		1.01	3.6	
1069			4779.16	39.5620	-113.8836	2012-08-09		0.73	3.9	Open water around casing
1079			4790.318	39.5320	-113.8848	2013-05-29		0.84	3.9	
1080			4788.409	39.5138	-113.8929	2013-05-29		-0.18	4.6	
61	SG25A	Yes	4789	39.5586	-113.8918			2.1	25	
62	SG25B	Yes	4789	39.5587	-113.8917			2.22	65	
63	SG25C	Yes	4789.1	39.5587	-113.8917			2.16	116	
64	SG25D	Yes	4795.1	39.5586	-113.8957			2.32	60	

Piezometers and wells shown on figure 1.
Wells have a two-digit site ID and piezometers have a four-digit site ID.

Table 2. *Metadata of predictor stations used for this study.*

Station ID	Station Name	Latitude	Longitude	State	Elevation (ft)	Network*	Measure Started	Data Frequency
USC00421144	Callao	39.8997	-113.713	UT	4342	GHCN	1902-11-01	Daily
USC00422607	Eskdale	39.1078	-113.953	UT	4980	GHCN	1966-03-01	Daily
USC00426708	Partoun	39.6308	-113.886	UT	4780	GHCN	1905-02-01	Daily
1147	Wheeler Peak	39.01	-114.31	NV	10120	SNOTEL	2010-10-01	Hourly
1247	Takka Wiiya	39.741	-113.9825	UT	9122	SNOTEL	2013-10-01	Hourly
10172870	Trout Creek	39.7441	-113.89	NV	6200	USGS	1986-10-01	Hourly
393345113503201	(C-14-18)26dbc-1MX			UT	4960	USGS	1981-08-23	Yearly

*GHCN data downloaded from the Utah Climate Center; SNOTEL data downloaded from USDA SNOTEL website.
Stations shown on figure 1.

at Leland Harris (see next paragraph). I specifically examined precipitation patterns, solar radiation, evapotranspiration, and soil moisture, which are also parameters measured by and derived from the local climate station that I deployed. I also downloaded gridded PRISM data (http://www.prism.oregonstate.edu/) and compared that with readings from the regional stations (see PRISM section of this report).

UGS Climate Station

In August of 2017, UGS employee Ethan Payne and I installed a solar-powered climate station at Leland Harris next to well SG25A (figures 1 and 2). The station is an Onset HOBO brand station, and it measures soil moisture, photosynthetically active radiation, temperature, humidity, barometric pressure, wind speed and direction, and precipitation as rain. The station includes all of the instrumentation necessary to estimate evapotranspiration using the Penman-Monteith method (Zotarelli and others, 2010). The station measures precipitation using a tipping bucket rain gauge, but it does not have a way to effectively measure snow accumulation. Unfortunately, the anemometer on this station malfunctioned on March 5, 2019, due to water penetrating the pulse adaptor, so there is a three-month gap in wind speed and direction data. Like the transducers in the wells and piezometers, the station is presently recording data.

Evapotranspiration Estimates

I used the UGS climate station data and the Penman-Monteith method to provide a localized estimate of potential evapotranspiration, one of the assumed driving forces of groundwater level changes in Leland Harris. To estimate the potential evapotranspiration, I used a step-by-step approach (Zotarelli and others, 2010).

To check the estimate, I also estimated actual evapotranspiration from hydrograph analyses of the piezometer data. Because the actual evapotranspiration data were derived from the piezometer data, I could not use it as one of the predictors for groundwater levels. However, it allowed me to establish a method to estimate evapotranspiration and potential recharge in the basin wetland systems. I applied techniques outlined in Fahle and Dietrich (2014) based on approaches by others (White, 1932; Hays, 2003; Loheide and others, 2005; Gribovszki and others, 2008). I aggregated those data into monthly intervals. Estimates of ET and recharge could allow for a better understanding of climatic controls on the surface-water/groundwater interaction.

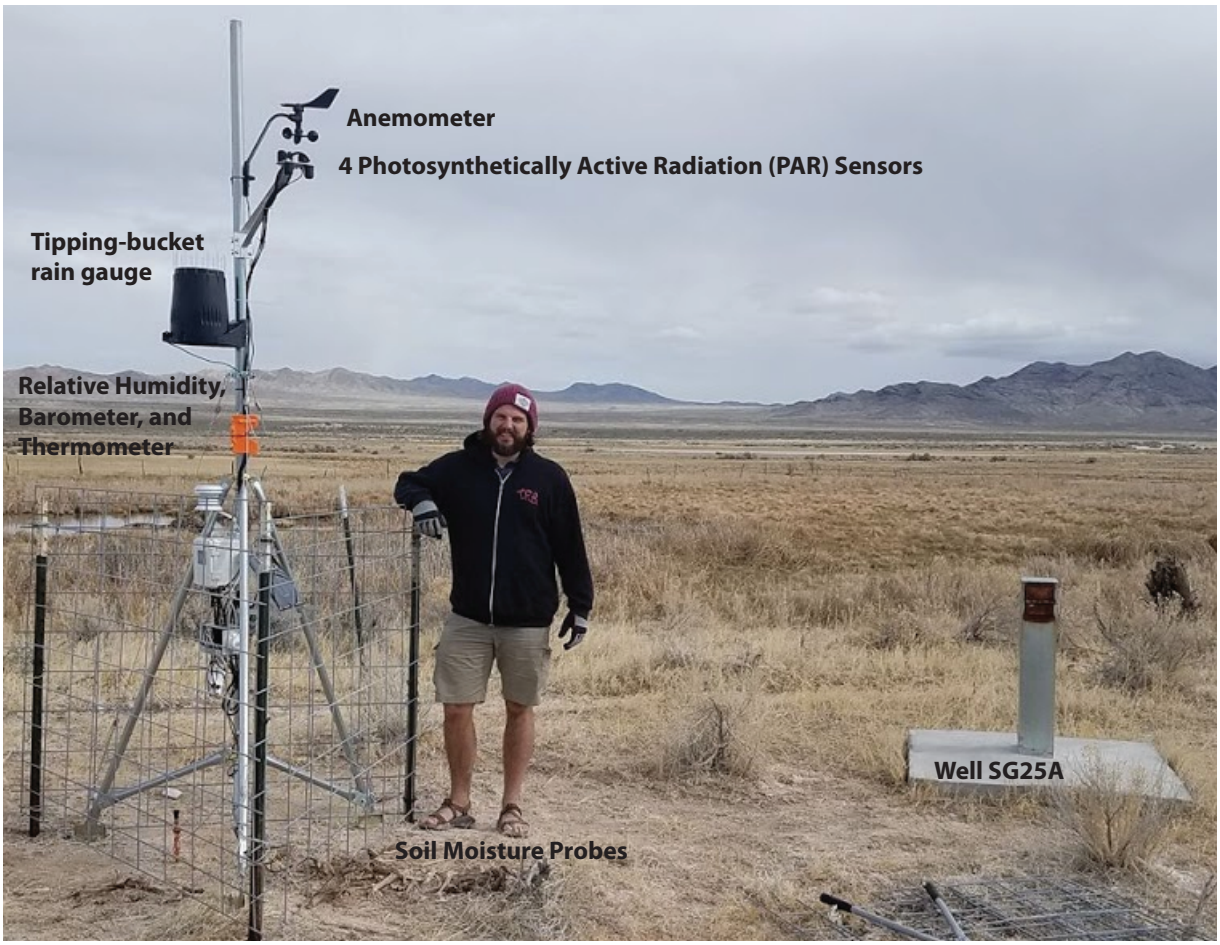

Figure 2. *UGS climate station at Leland Harris, with the major components labeled.*

PRISM Data

A team at Oregon State University developed an algorithm that accurately interpolates data from climate stations, specifically precipitation, temperature, and vapor pressure. The algorithm is called PRISM, Parameter-elevation Regressions on Independent Slopes Model, because it uses spatial regression to account for slope, aspect, and elevation when interpolating. I used the PRISM Data Explorer tool (http://prism.oregonstate.edu/explorer/) to download daily precipitation, temperature, and vapor pressure data from 2000 to 2019 for the location of SG25A. This download consisted of interpolated four-kilometer grid cells from the most current PRISM dataset (PRISM Climate Group, 2019).

Local Climate Stations

While I initially examined data from 15 climate stations in the Snake Valley region, I settled on using data from five regional weather stations: Partoun, Eskdale, Callao, Wheeler Peak, and Takka Wiiya (figure 1; table 2). These five stations were selected based on proximity to Leland Harris and the completeness of their time-series data relative to the other stations. Because it has a complete climate record and is the closest station to Leland Harris, I used the Partoun station when conducting cross correlations. In terms of groundwater gradient relative to Leland Harris, Partoun, Wheeler Peak, and Eskdale are all upgradient of the wetland complex. Upgradient precipitation and snowmelt is assumed to have a more significant hydrologic impact on the site, as these are the probable points of recharge for the site.

Temporal Analysis

Correlation

As an exploratory precursor to conducting modeling of the groundwater levels, I conducted correlation analyses between the predictors and the water level data. I attempted to describe the driving forces of the groundwater level changes using cross correlation and correlation matrices. To prepare for this analysis, I conducted an augmented Dickey-Fuller analysis on time series for each piezometer, as well as the adjacent spring gradient wells (SG25). Most of the data failed the Dickey-Fuller test for stationarity (Dickey and Fuller, 1979). Stationarity is a measure of how consistent the variance of the data is over time. Many of the groundwater hydrographs have variance that changes seasonally, meaning that the time series must be normalized prior to performing regression. I normalized the data in all the wells and the predictor data using the first difference technique, where the following value is subtracted from the preceding value in a time series (n[i] - n[i-1]). First difference is a measure of the change over time (units of length per sample frequency). Second difference is the first difference of the first difference, which is a measure of the rate of change over time. First and second difference can be applied if the data show a high autocorrelation, where the data time series correlates with a lagged version of itself, which was the case for many of the datasets analyzed.

I cross correlated all of the examined groundwater levels against precipitation, evapotranspiration, stream flow, and temperature. Cross correlation consists of offsetting one time series by a specified number of time steps (lags) and then conducting a Pearson correlation analysis against the offset dataset. The algorithm I used normalizes the data on input by default. The resulting output will show the correlation coefficient for each lag, including no lag, up to the specified offset. Cross correlation can help diagnose a lag between an influencing variable and groundwater level. For the cross correlations against precipitation and evapotranspiration, I separated the time series into two segments, winter and not winter, to segregate snow-driven hydrology from evaporation-dominated hydrology. I conducted a cross correlation between hourly Trout Creek (USGS Station 10172870) flow data and the hourly water level data, using the second difference of both series as the input, examining lags of 3 days and 3.5 years.

Decomposition and Fast Fourier Transform

I analyzed the periodicities and long-term trends in the groundwater elevation data to determine if there are consistent long-term trends and frequencies between the datasets. I conducted Fast Fourier Transform (FFT) on all the groundwater elevations. FFT uses combinations of sine waves to determine the dominant frequencies and their amplitudes in a dataset. The result is a plot with frequency on the x axis and amplitude on the y axis, showing prominent spikes in amplitude for each relevant frequency within the dataset. Several hydrologists have applied frequency analyses like FFT to better understand trends and driving factors in water level data (Inkenbrandt and others, 2005; Foster, 2007).

To better visualize the long term and seasonal trends in groundwater levels, for each piezometer and well hydrograph, I conducted a seasonal decomposition. I used the seasonal decomposition tool in the statsmodels Python library (Seabold and others, 2010) to conduct the decomposition. The tool uses naïve decomposition, that uses additive moving averages and convolution filters to separate the hydrographs into their major component trends. The output consists of seasonal, trend, and residual components. The user enters the frequency of the yearly component to be removed, which for the case of the hydrographs was determined to be one year based on FFT and harmonic analyses.

Harmonic Analyses

I examined and compared the repeating patterns in water level time series to evaluate the driving forces of those patterns.

Wavelet analysis allows for the measurement and comparison of nonstationary data—data whose variance and frequencies may change over time. I applied wavelet transform analysis to examine the influence and phase coherence of potential predictor time series of the wetland piezometer data. All analyses were conducted using the Waipy Python library by Mabel Calim Costa (https://wavelet-analysis.readthedocs.io/en/latest/index.html). First datasets were normalized, then they were analyzed with a continuous wavelet transform using the Morlet wavelet. The continuous wavelet transform produces a plot showing the magnitude and frequency of a time series over time, like the results of FFT. Once each transform was conducted, I applied Cross Wavelet Analysis (CWA). CWA is a technique that compares continuous wavelet transforms from two time series to see if the same periodicities exist in both datasets. The output also shows if the datasets are in phase (not lagged) or out of phase (lagged) relative to each other. I used a Python Waipy method derived from Maraun and Kurths (2004). Finally, I generated coherence plots to compare the alignment of phases and the amplitude of that alignment for each CWA.

Modeling

I modeled groundwater levels at Leland Harris as an attempt to better understand the controlling variables and seasonality in the data and to predict impending changes. I used two different modeling platforms, both operated using Python: PASTAS (Collenteur and others, 2019) and Prophet (Taylor and Letham, 2017).

PASTAS (Collenteur and others, 2019) is specifically designed for the analysis of hydrological time series. It uses an additive combination of stress models to reproduce the modeled hydrograph (Collenteur and others, 2019). Each stress model is based on a hydrologic stressor, such as evapotranspiration, precipitation, or pumping. The stress models use sums of distributions, such as gamma and exponential distributions, with tuning parameters to facilitate the match to the groundwater elevation data. Similar models have been applied by others for modeling groundwater levels (van Geera and Zuur, 1997; von Asmuth and others, 2002, 2007). I used temperature, the reference evapotranspiration estimate provided by the climate station, and precipitation as the stressors and the Gamma and Hantush distributions for the PASTAS analyses. The models were run first by using individual stressors, then combinations of ET and precipitation from the Partoun climate station (table 2).

Prophet is a time series modeling library developed by the social media platform Facebook to predict and analyze time series data. Prophet uses a generalized additive model that sums various scales of seasonality detected in the modeled dataset (Taylor and Letham, 2017). Prophet does not require multivariate data to generate forecasts and accepts data having gaps. Prophet is scalable and rapidly applicable. I ran the Prophet model on all the piezometers and the wells, both with and without the use of additional predictor data (regressors). The regressors examined for the Prophet models were maximum temperature, evapotranspiration, and precipitation at Partoun, and discharge of Trout Creek (table 2). To check the fit of the Prophet models, I separated the water level data into training data and test data using the beginning of 2017 as the cut-off point. The model was fit using the training data, and model fit measures were calculated using the test data.

Elevation Analysis

I examined the bathymetric data provided by Grover, along with lidar (Light Detection and Ranging) data of the Snake Valley wetland systems. The lidar data are derived from airplane-mounted lasers that measure the distance between the plane and various reflectors, including the ground (bare earth) and vegetative canopy. The laser repeatedly fires creating an elevation point for each distance measurement, allowing for penetration through vegetation, but not through water. Richard Emerson, former employee of the UGS, informed us that the lidar mission in Snake Valley was flown during July or August of 2009. The summer acquisition time of the lidar data coincided with low surface water levels, increasing the amount of usable elevation data for the wetland systems. Based on measurements with a high precision GPS unit in 2011, the vertical accuracy of the lidar data is within ± 0.1 meter, except in areas of dense vegetation, where the accuracy is lower (Richard Emerson, verbal communication, 2019). The minimum usable elevation of the lidar data is 1456 meters. This elevation represents the elevation of the water surface in the larger and deeper pools at the time of acquisition. The data were collected at a horizontal resolution of 1 meter.

In April and May of 2013, Grover conducted a bathymetric survey consisting of 3852 measurement locations, and conducted repeat measurements at 47 sites distributed throughout Leland Harris (Grover, 2016). I attempted to match his measurements to the lidar data. Grover's repeated water-depth measurements consisted of measuring the distance from the tops of submerged static metal poles to the water surface, whereas his bathymetric survey consisted of measuring the water depth from the bottom of the pool and from the bottom of soft sediment to the water surface. I estimated pole lengths (distance from bottom of pool to top of pole) of all the measurement points based on data from the bathymetric survey and estimated the pole-top elevations using the sum of pole length and the lidar data. If a pole was submerged during the summer, I calculated the water elevation of a nearby pole in the same patch (pool) and back-calculated the pole-top elevation. Using the estimated pole-top elevations and the water-depth measurements, I calculated water-level elevations at the measurement poles over time. I interpolated the measurements to estimate the wetland-wide water-surface elevation for each month of measurement.

Using the lidar data, I created a hypsometric curve for Leland Harris. A hypsometric curve shows the relationship between the elevation of the water surface and the area inundated or the volume of water inundating that area. First, I clipped the lidar data to include only the Leland Harris wetland system, excluding the adjoining playas to the east and highlands to the west. I created a series of constant elevation rasters incrementing 0.01 meters. Then I conducted a cut-fill analysis of the lidar data against each constant elevation. Cut-fill analysis outputs the areas and volumes of change between two surfaces. I then tabulated the volumes and areas from each cut-fill analysis output.

RESULTS AND DISCUSSION

General Trends

All the piezometer and well water levels examined had similar seasonal trends (figure 3). Maximum water level elevations occurred in mid- to late February (figure 4). From February to late March, the water levels declined. In most of the piezometers and wells, the water levels stabilized from March to late May. In late May, usually around the 20th, the water levels in the piezometers declined, having the greatest negative slope from this time until July (table 3). Many of the piezometer water levels had a notable slope change in July, where the slope generally decreased but stayed negative. Lowest average water levels occurred near mid-August, after which time the water levels began to rise. This rise was the greatest positive slope of the piezometer data, which leveled off in mid-October and had a final sharp rise in late December.

There are notable variations in water levels related to variations in annual precipitation. Water year 2011 (Oct. 2010 to Sept. 2011) had the greatest measured precipitation for all the climate station data, showing an annual sum of about 12 inches (30.5 cm) of precipitation in the valley and 55 inches (140 cm) of snow-water equivalent at Wheeler Peak (figure 5). The general trend for all examined water levels shows a consistent decrease since 2012, with a slight increase at the beginning of 2019 (figure 6). Comparing the standardized water elevations against climate shows a lag between peak precipitation and peak groundwater level (figure 6). This lag is discussed in greater detail in the Correlation section. Calendar years 2017 and 2018 showed some of the lowest minimum yearly water levels with the seasonal May drops occurring earlier in all the spring gradient wells and most of the piezometers — 1011, 1012, 1013, 1014, and 1015 (figure 4). Calendar years 2011 and 2012 had some of the highest minimum yearly water levels (least amount of yearly decline) during the August low period (figure 4). These years also showed a delayed May decline relative to the other years (figure 4).

Differences in long-term variation in groundwater elevation and temperature could indicate relative influence from surface water. Piezometer 1012 had the least amount of total variation in both temperature and water level and the highest mean temperature and groundwater elevation, which could be attributed to a closer connection to the groundwater system and less connection to the surface water system (table 4). Piezometers 1014, 1015, and 1016 had some of the highest standard deviations in both temperature and water elevation, which could indicate a strong surface influence.

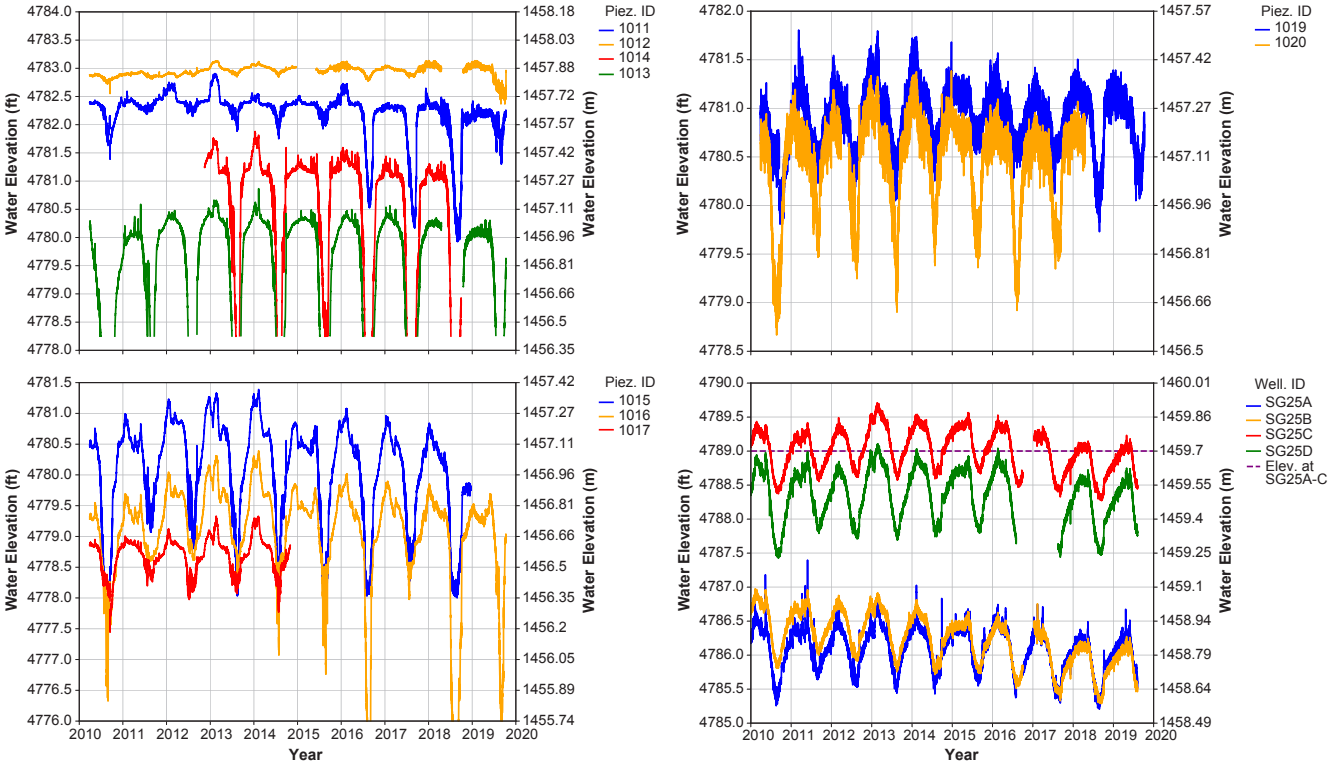

Figure 3. *Hydrographs of piezometers and wells examined for this study.*

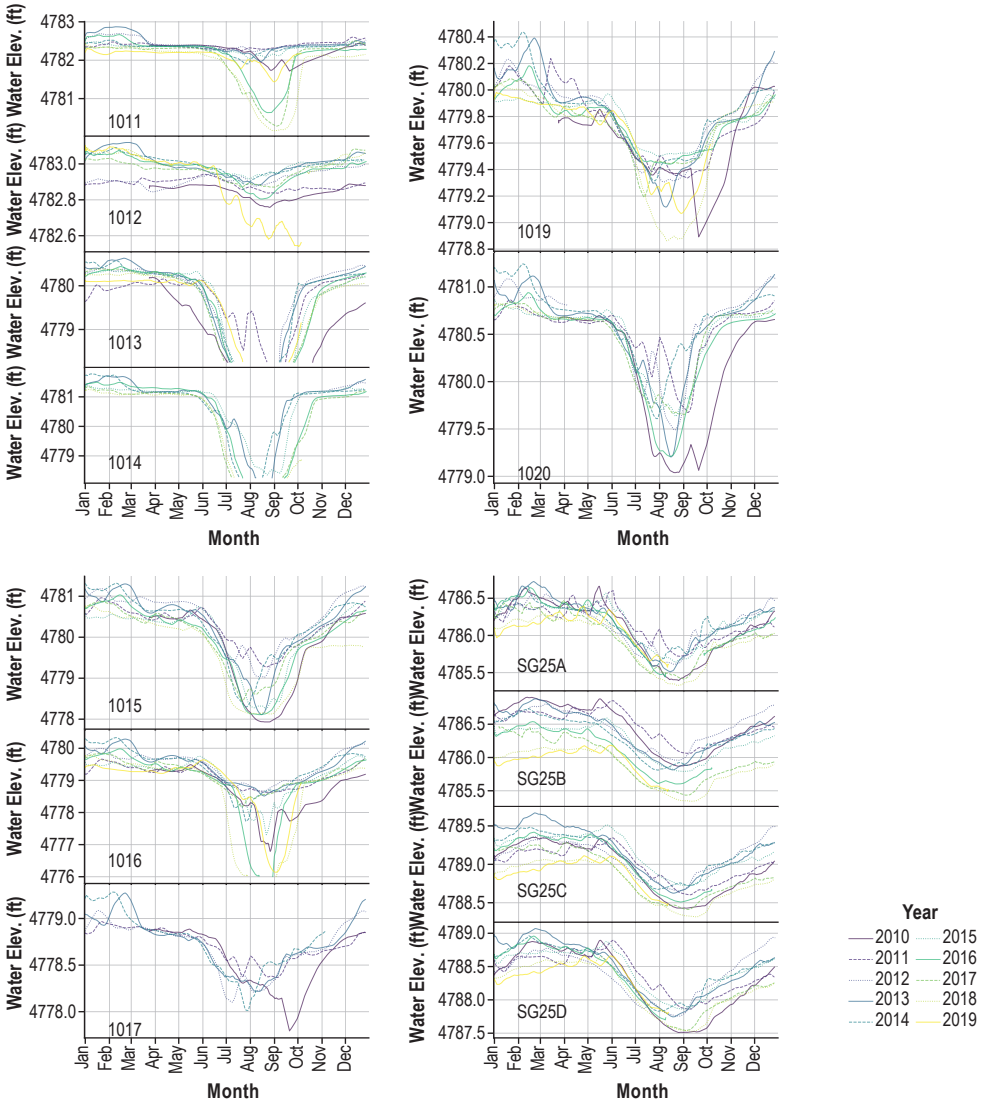

Figure 4. *Yearly hydrographs of the wells and piezometers examined for this study.*

Table 3. *Dates of average water-level-trend changes.*

Well	Max	Spring Flattening	Main Drop Start	Low Step	Min	Fall Flattening	Winter Climb
SG25A	Feb 14	Mar 21	May 20	Jul 19	Aug 18	Oct 12	Dec 21
SG25B	Feb 21	Mar 21	May 20	Jul 26	Aug 28	Oct 12	Dec 21
SG25C	Feb 27	Mar 21	May 20	Jul 27	Aug 30	Oct 12	Dec 21
SG25D	Feb 27	Mar 21	May 21	Jul 19	Aug 28	Oct 12	Dec 21
1011	Feb 10	Mar 29	May 21	Jul 14	Aug 28	Oct 12	Dec 16
1012	Feb 07	Apr 08	May 23	Jun 29	Aug 23	Oct 17	Dec 08
1013	Feb 11	Mar 21	May 20	Jun 27	Aug 28	Oct 17	Dec 21
1014	Feb 07	Mar 13	May 20	Jul 07	Aug 13	Oct 25	Dec 21
1015	Feb 09	Mar 21	May 24	Jul 17	Aug 13	Oct 12	Dec 21
1016	Feb 09	Mar 21	May 22	Jul 24	Aug 28	Oct 17	Dec 21
1017	Feb 09	Mar 21	May 20	Jul 07	Aug 03	Oct 19	Dec 21
1019	Feb 09	Mar 24	May 23	Jul 14	Aug 18	Oct 15	Dec 21
1020	Feb 09	Mar 21	May 23	Jul 19	Aug 18	Oct 15	Dec 21
Average	Feb 13	Mar 22	May 21	Jul 14	Aug 21	Oct 15	Dec 19

“Max” and “Min” are the dates of the yearly maximum and minimum values, respectively.
"Spring flattening" refers to the water levels asymptotically leveling off after decreasing from the yearly maximum.
“Main Drop Start” is when the water levels start to drop dramatically in spring.
“Low Step” refers to flattening near the minimum value.
“Fall flattening” refers to water levels flattening off after increasing in the fall.
“Winter climb” is the increase to the yearly maximum.

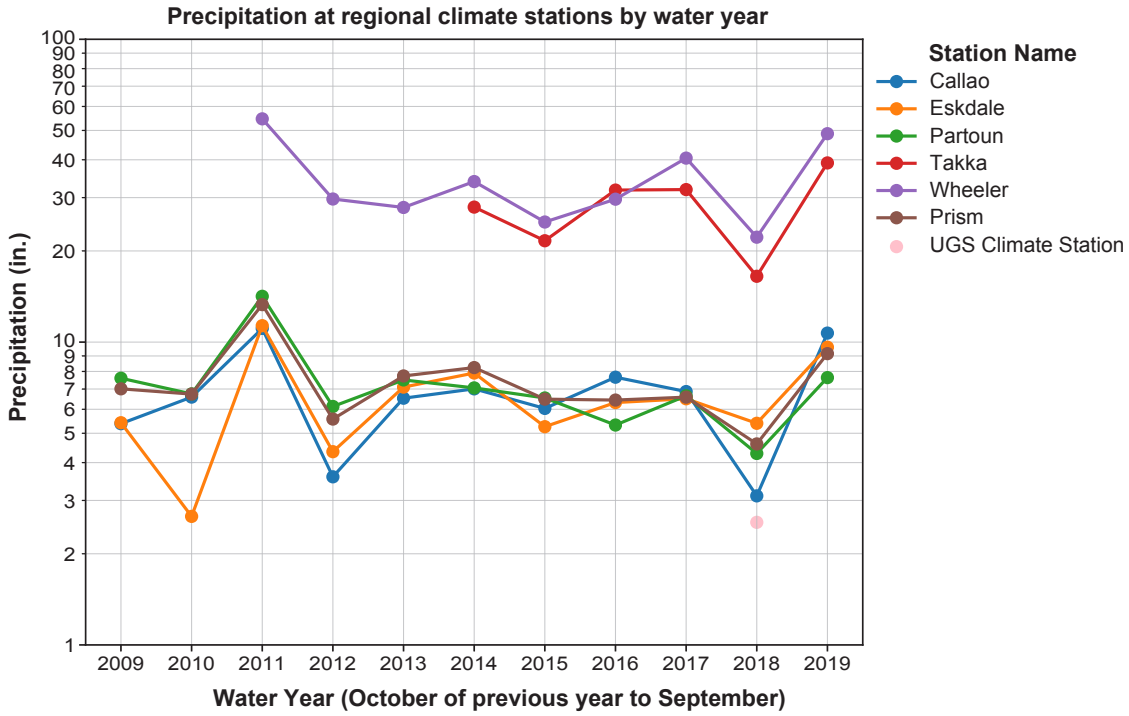

Figure 5. *Yearly total precipitation at the weather stations monitored for this study. See figure 1 for station locations.*

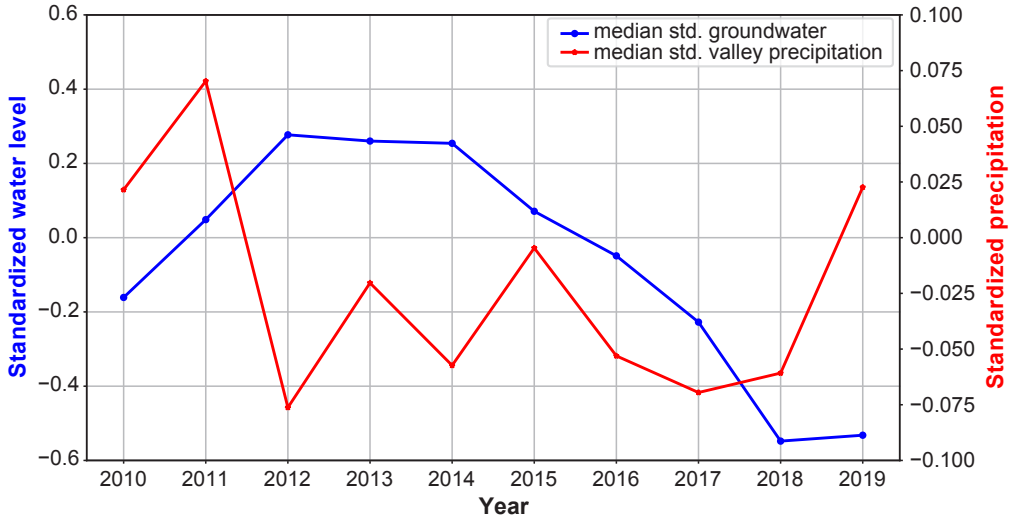

Figure 6. *Median standardized yearly groundwater level of the Leland Harris piezometers and median standardized precipitation of the regional climate stations presented in figure 5.*

Data from the spring gradient wells should reflect the groundwater conditions contributing to the Leland Harris system, and trends at the SG25 wells are like those observed in most of the wetland piezometers. All the spring gradient wells show a long-term general increase in temperature. SG25D has a much lower variance in water level and temperature. It shows a lagged offset of temperature relative to the other spring gradient wells, although this same lag is not apparent in the water-level data. The differences in gradient and lag in timing likely reflect conditions in the wellbore more than conditions in the aquifer, as SG25D has a greater depth to water than SG25A to C. The well data show that water elevation head increases with well screen depth, which indicates an upward hydraulic gradient, consistent with the obvious groundwater discharge at Leland Harris. SG25A and B appear to have undergone a gradient reversal starting in summer of 2017, where groundwater elevation head in SG25B is now persistently lower than SG25A (figure 3). This may be from buffering created by pulling from the water storage in the surface wetland system. Comparison of long-term groundwater trends in the decomposition data show a more precipitous drop in water levels at SG25B data from 2010 to 2019 than in the other wells, including the deeper wells, which could indicate some type of preferential dewatering of the aquifer materials at the depth of the screened interval of SG25B (figure 7).

Table 4. *Summary statistics of water level and temperature data collected by transducers in piezometers and wells examined for this study.*

Data Type	Well	Count	Mean	Std. Dev.	Min	25%-tile	Median	75%-tile	Max	Range
Temperature	SG25A	82641	11.7	2.91	7.1	9.10	11.20	14.40	17.10	10.05
	SG25B	81591	11.7	3.14	6.6	9.00	11.00	14.70	17.40	10.85
	SG25C	81593	11.3	3.23	5.8	8.60	10.70	14.30	17.10	11.35
	SG25D	74991	12.3	0.69	10.9	11.70	12.17	12.80	13.79	2.89
	1011	83487	8.5	2.95	4.4	5.90	7.50	11.20	30.00	25.60
	1012	75041	11.9	1.95	7.2	10.10	12.00	13.60	16.00	8.80
	1013	79147	10.9	3.97	4.4	6.90	10.40	14.90	21.90	17.50
	1014	51119	7.6	3.26	2.6	4.60	7.00	11.10	13.40	10.80
	1015	76430	10.8	4.00	4.8	6.90	10.40	14.60	26.40	21.60
	1016	83490	10.2	3.11	5.5	7.10	9.90	13.20	47.80	42.30
	1017	40240	9.9	2.87	5.9	7.20	9.50	12.60	15.00	9.10
	1019	83561	8.0	3.01	3.5	5.40	7.30	11.00	13.60	10.10
	1020	68898	11.2	3.34	6.1	8.00	10.80	14.50	16.50	10.40
Water Elevation	SG25A	82693	4786.1	0.31	4785.2	4785.89	4786.16	4786.35	4787.40	2.19
	SG25B	81591	4786.2	0.36	4785.3	4785.97	4786.26	4786.52	4786.98	1.69
	SG25C	81593	4789.0	0.30	4788.3	4788.77	4789.04	4789.26	4789.71	1.44
	SG25D	74991	4788.4	0.38	4787.4	4788.06	4788.43	4788.67	4789.11	1.68
	1011	83487	4782.2	0.43	4779.9	4782.20	4782.33	4782.39	4782.91	2.98
	1012	75041	4782.9	0.09	4782.4	4782.89	4782.96	4783.01	4783.14	0.77
	1013	61821	4780.0	0.49	4778.3	4779.88	4780.14	4780.29	4780.87	2.62
	1014	44004	4780.9	0.73	4778.3	4780.95	4781.14	4781.24	4781.88	3.63
	1015	76430	4780.1	0.82	4777.9	4779.71	4780.35	4780.65	4781.39	3.51
	1016	81550	4779.2	0.68	4776.0	4778.90	4779.31	4779.59	4780.39	4.39
	1017	40240	4778.7	0.28	4777.4	4778.52	4778.75	4778.88	4779.33	1.89
	1019	83561	4779.7	0.29	4778.6	4779.53	4779.80	4779.93	4780.51	1.92
	1020	68898	4780.5	0.46	4778.7	4780.35	4780.66	4780.75	4781.37	2.70

Piezometers and wells shown on figure 1.

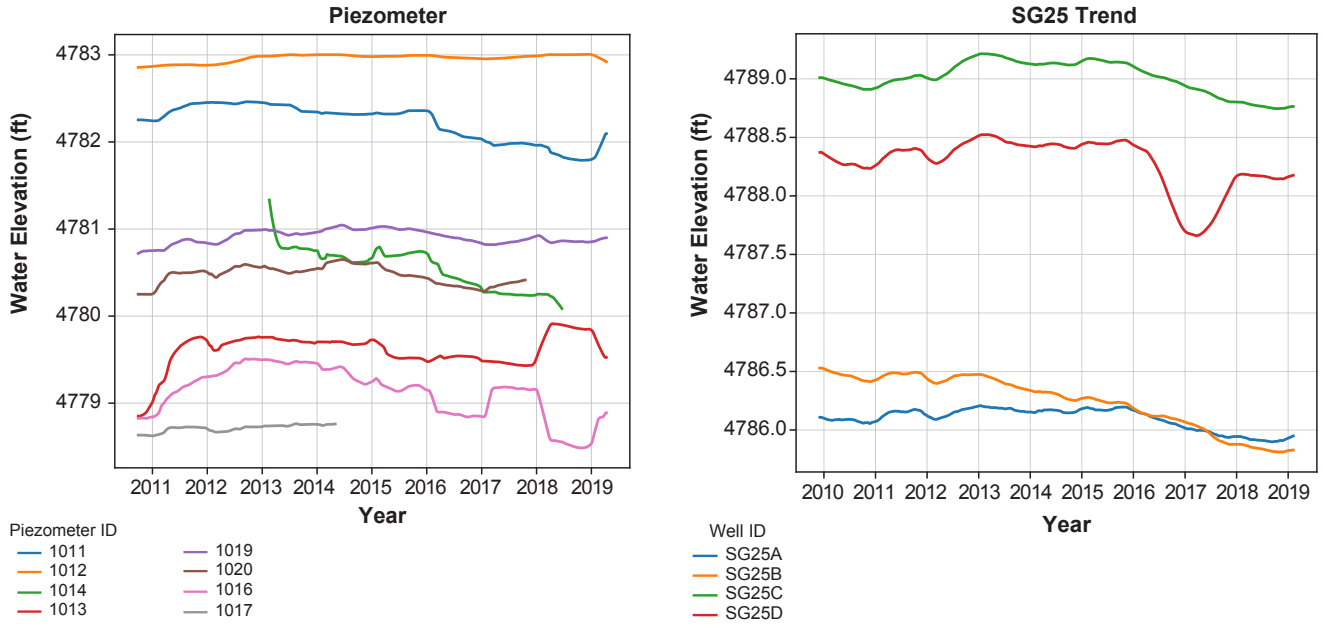

Figure 7. *Trend data extracted using decomposition analysis.*

Daily variation in water level is important to consider when aggregating daily data to hourly data and the timing of manual measurements. Daily variation in the water level data show that groundwater levels peak during 7 to 9 a.m. and then are at their lowest during 5 to 7 p.m. (figure 8). However, the median daily range of fluctuations is only about 0.6 inches (1.5 cm) at most. The greatest observed variation was in well 1016 with a range of about 1.5 feet (figure 8). However, this high range was an outlier, whereas more than 75% of the daily ranges in 1016 were below 0.48 inches (1.2 cm). Piezometers 1014 and 1015 showed the greatest average daily variation. Like overall variation, 1012 had the lowest daily variation. Based on the relatively small, but measurable changes observed in the daily data, aggregating the data by mean to daily data would not cause significant bias.

Evapotranspiration Estimates

Hydrograph-based ET estimates seemed realistic relative to the reference ET estimates calculated from the Partoun weather station (figure 9). The Hays (2003) and White (1932) techniques generate evapotranspiration values lower than Partoun reference ET (figure 9A and B, respectively), while the Gribovszki (2008) approach generates ET values very close to the reference ET (figure 9c). However, there appear to be many outliers in the dataset, likely created by non-evapotranspiration-derived groundwater level changes like those resulting from precipitation events. After applying filtering to the precursor data and post-estimate rolling window smoothing, estimates of actual evapotranspiration from the hydrographs were very realistic matches of the reference ET (figure 9d). Annual evapotranspiration estimates ranged from 10 inches (25 cm) per year to 55 inches (140 cm) per year (figure 10). The Gribovszki (2008) technique showed the greatest ET values and ranged from 35 to 55 inches (89 to 140 cm) of annual ET (figure 10). The White (1932) technique yielded the least amount of ET, mostly staying below 20 inches (51 cm) per year (figure 10). Based on the estimates, ET peaks in July and August and diminishes to near zero from November to February (figure 10). The results compare well to estimates from Hill and others (2011), which are specific to wetlands of the Delta area. The Hill and others (2011) data show no ET from November to May, and show a sharp peak in the summer months with an apex in August. The data trends for open water from Hill and others (2011) are flatter and more persistent over the year, and a mix of the two datasets would be similar to the estimates at Leland Harris. Of the three techniques applied for the hydrograph analysis approach (White, 1932; Hays, 2003; Gribovszki and others, 2008), the Gribovszki (2008) approach had the best match to the reference evapotranspiration estimated at Partoun (figure 10). It is worth noting that the reference ET may not be representative of values that would be expected for a wetland complex in this area, as reference ET is based on a standard crop ET rate and not the ET rate of wetland plants. Based on the comparison of the different datasets, the Gribovszki (2008), Hays (2003), Hill and others (2011) methods are relatively representative of the ET at Leland Harris, while the White (1932) approach appears to underestimate the total ET.

Correlation

A statistically significant (95% confidence interval) correlation exists between precipitation at Partoun and groundwater levels at Leland Harris. A significant same-day correlation exists in all the hydrographs analyzed. A one-day lag is persistent across all hydrographs analyzed, and is most prominent in piezometers 1012, 1014, and in spring gradient well SG25C (figure 11). Stations 1014, 1017, 1020, and all of the SG25 wells show a small but statistically significant correlation to an 18-day lag (figure 11). Having both one- and two-day correlation values could indicate attenuation and delay in the rain signal, where it has both immediate effects and delayed effects on the surface water system. Whereas this type of correlation is also common in autocorrelated signals, autocorrelation is unlikely due to first-differencing prior to analysis.

Longer term lag from precipitation-driven recharge is harder to discern from the correlation analysis, but an analysis between USGS Well 393345113503201 and Partoun precipitation indicates that there may be a three-year lag between long-term water levels and precipitation (figure 12). A notable offset in peaks between the detrended water level data and the precipitation and flow records, specifically the 2011 water year, also suggests that a three-year lag may exist.

Mountain stream flow can be a good proxy for snowmelt and subsequent groundwater recharge, as it signifies the timing and abundance of snowmelt. The cross correlation between hourly Trout Creek discharge and the hourly water-level data reflects the weak correlation observed between water level and multi-year lags of precipitation data. Lags of 8 hours to 2 days produced significant positive correlations between flow and groundwater levels, though the correlation coefficient was less than 0.02 in those cases. Data from stations 1013, SG25A, and SG25B have significant correlation to flow at 2.3-year lags (figure 13). Piezometers 1011, 1014, 1016, and 1019 show a prominent correlation around the 1.75-year lag, which reflects the correlation observed in the long-term groundwater level data and Partoun precipitation (figure 14).

Groundwater age data from Hurlow (2014) show that water from the spring gradient wells at Leland Harris contains less than 0.07 TU of tritium and at most 30.81 percent modern carbon, indicating that the water from those wells has likely traveled through the groundwater system for more than 50 years and a component of that water is likely much older. The response and delay observed in the time series data are likely the result of a pressure response in groundwater levels, and do not represent the actual travel time of a water molecule from recharge point to discharge point.

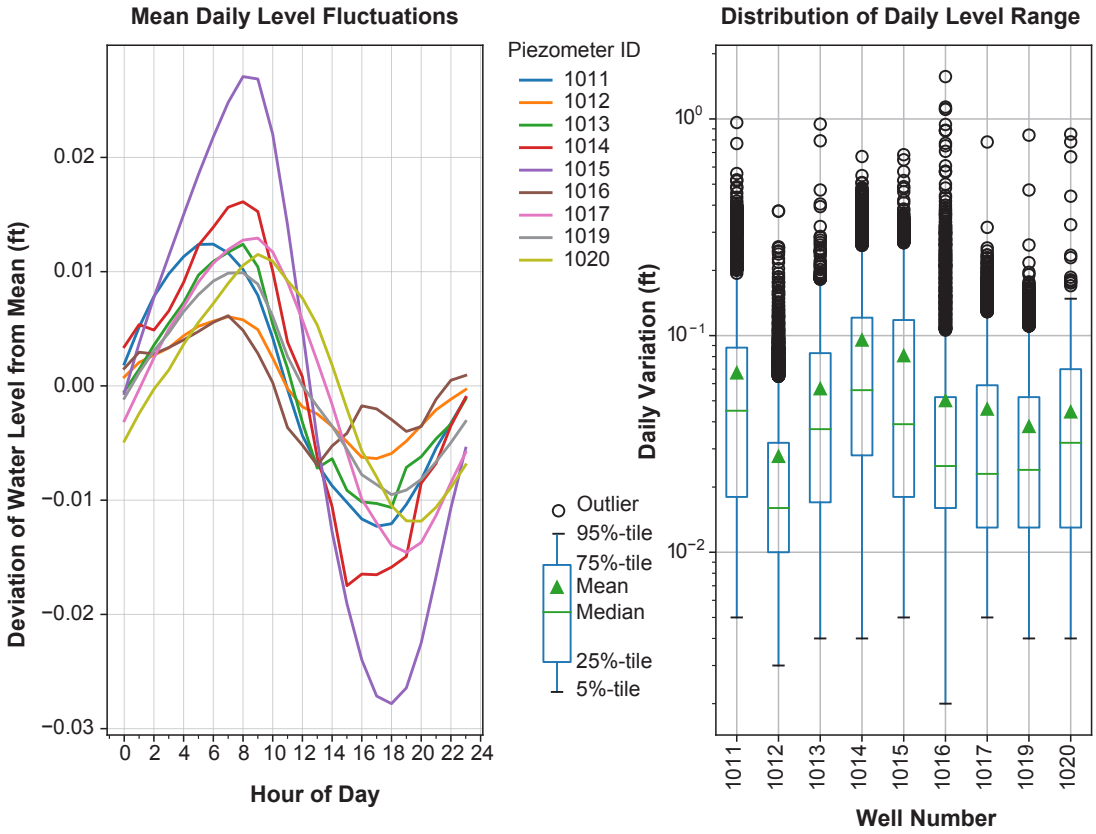

Figure 8. *Daily variation water levels of Leland Harris piezometers.*

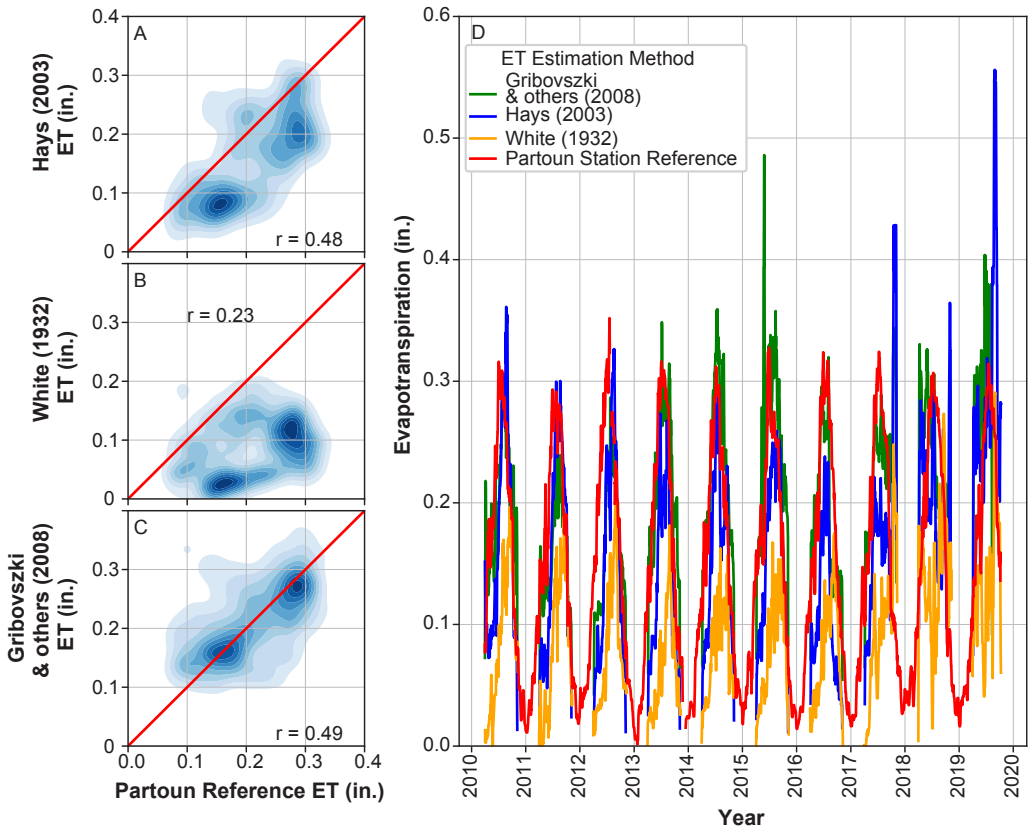

Figure 9. ***(A–C)*** *show the densities of scatter points with a red line indicating a one-to-one relationship, and where darker zones are higher densities.* ***(D)*** *is a comparison of piezometer-estimated evapotranspiration rates to reference evapotranspiration estimated at the Partoun weather station.*

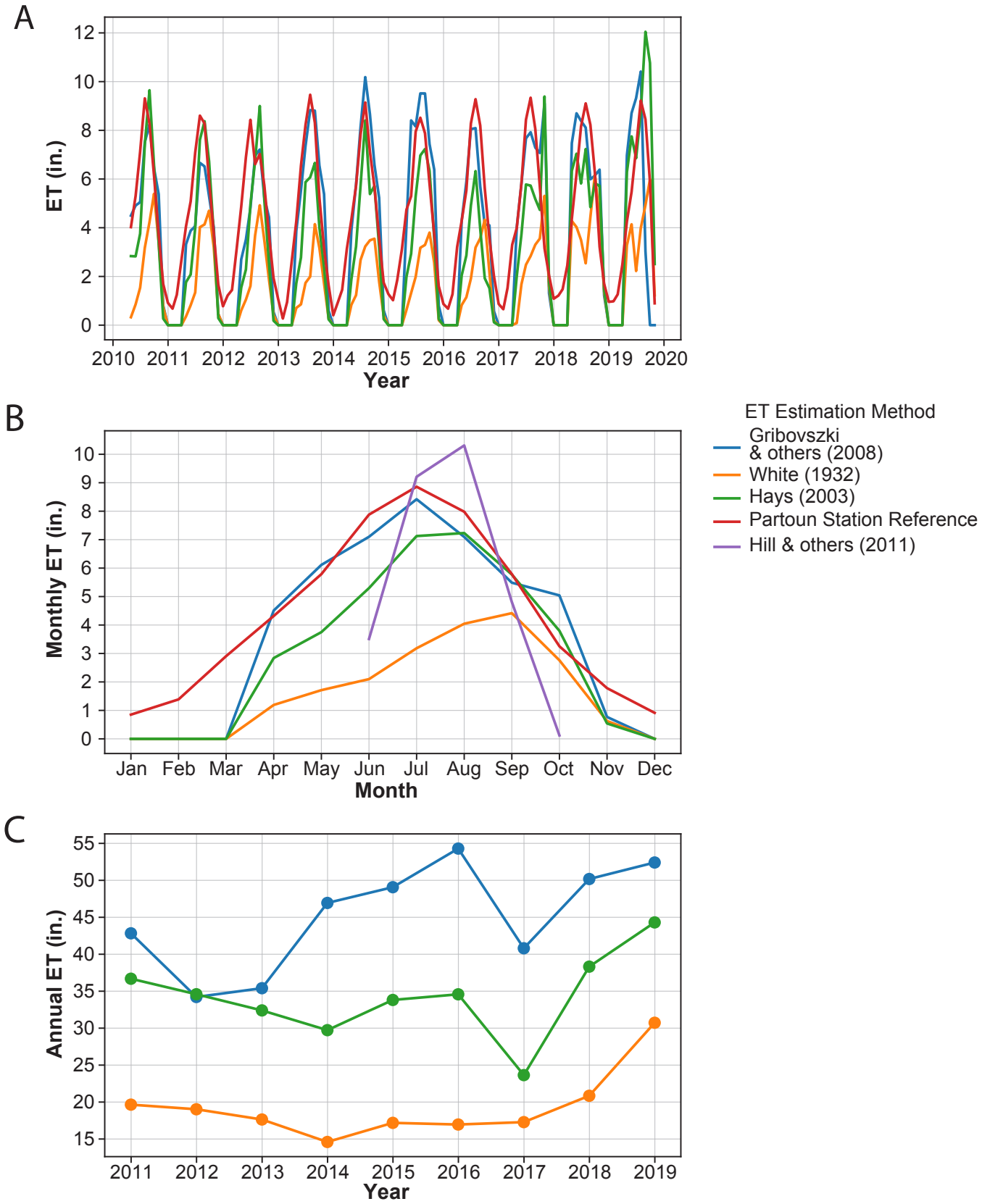

Figure 10. *Total* ***(A)****, monthly* ***(B)****, and annual* ***(C)*** *evapotranspiration estimated by different methods compared to the reference evapotranspiration at Partoun and wetland reference evapotranspiration at Delta by Hays (2003).*

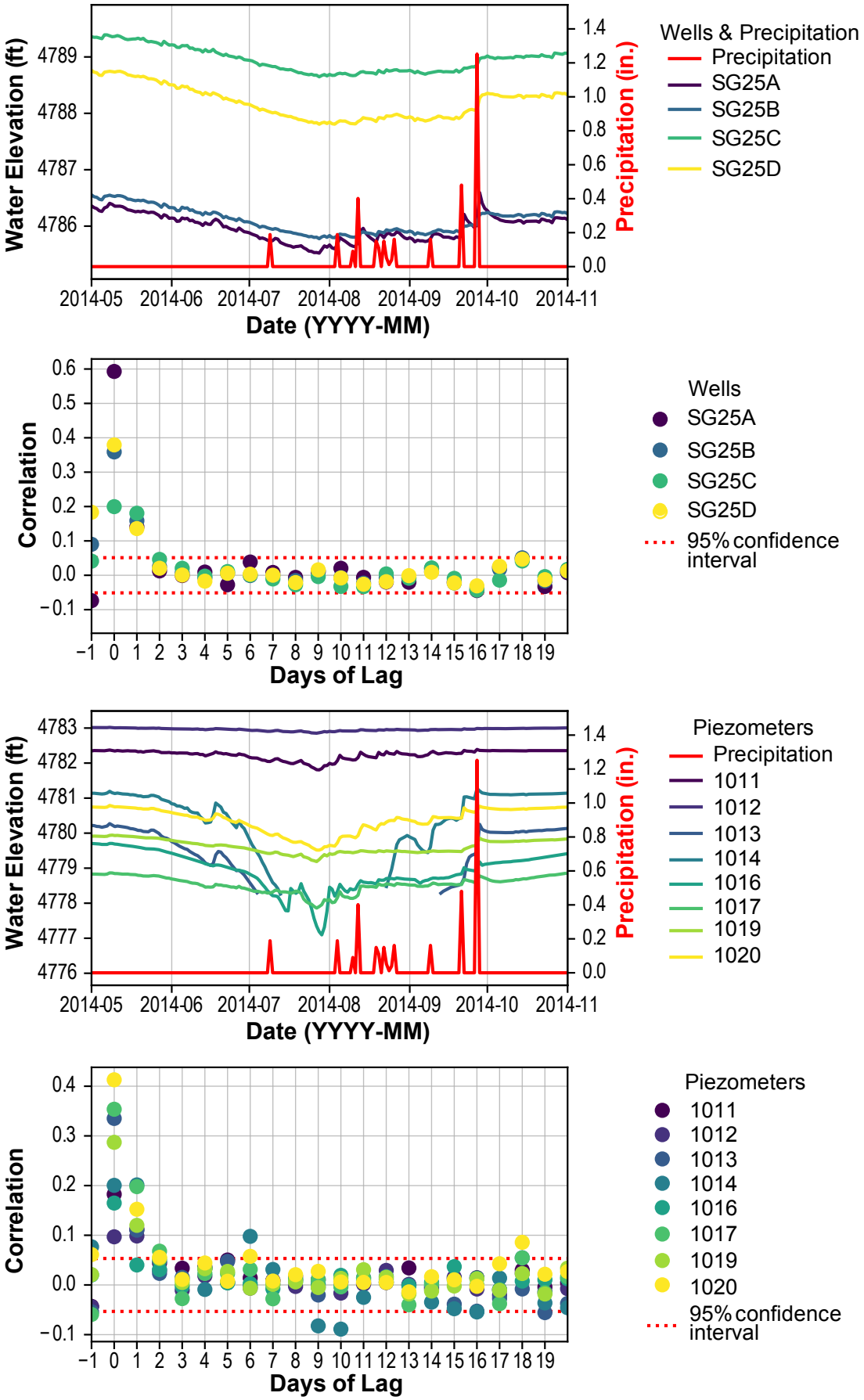

Figure 11. *Cross correlation between precipitation and water level elevations.*

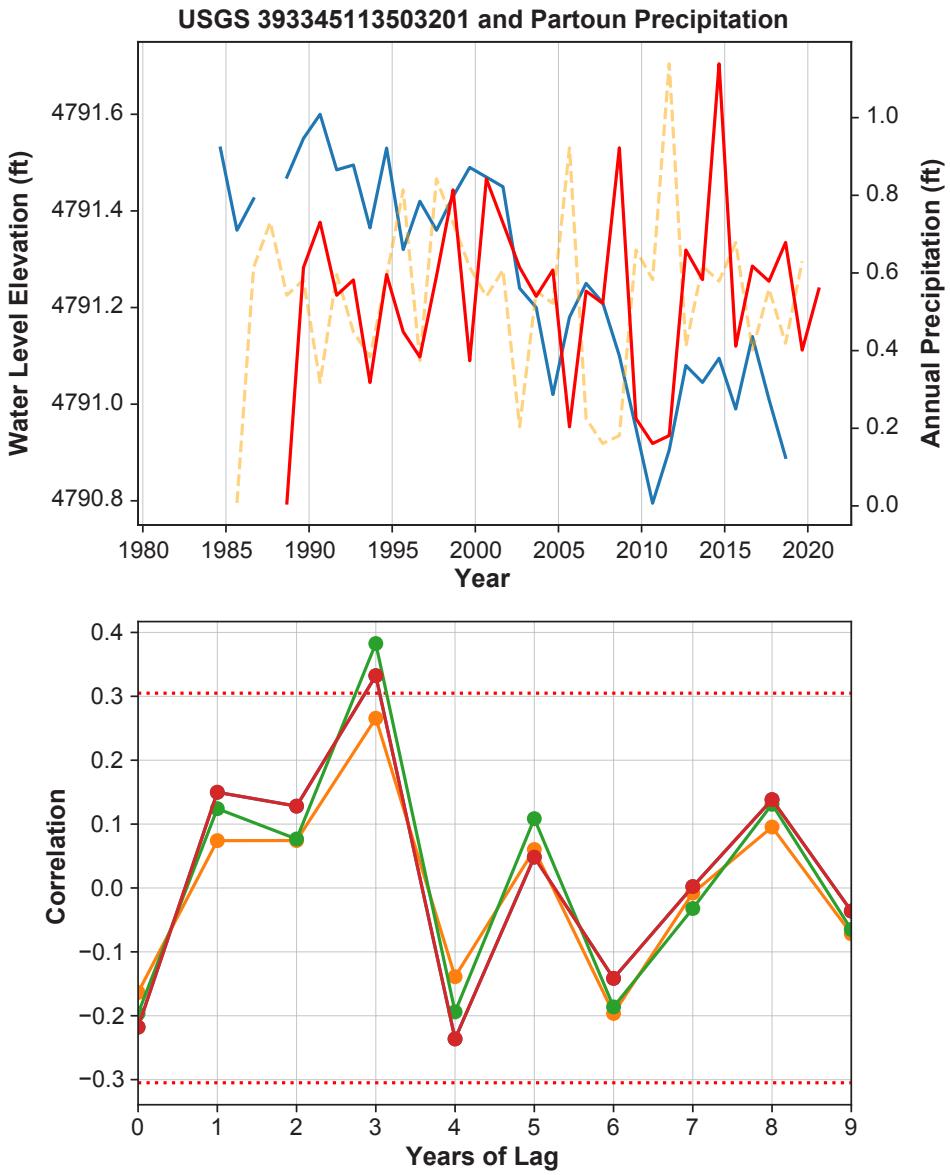

Figure 12. *Cross correlation between precipitation and long-term water levels.*

It is worth noting that correlation between discharge in Trout Creek and groundwater levels in Leland Harris does not necessarily indicate a direct hydraulic connection. The timing of the snowmelt from the Deep Creek and Snake Ranges is likely similar for all streams along the north-south trending mountains, and flows measured in Trout Creek are likely similar in fluctuation to flows along those mountain ranges. Potentiometric surface maps and conceptual groundwater flow diagrams indicate that the outflow of the creek is downgradient of Leland Harris, meaning that it likely does not have a direct influence of groundwater levels (Gardner and others, 2011; Hurlow, 2014).

Harmonics

FFT analysis resulted in prominent frequencies of 1 and 2 cycles per day and 1 and 2 cycles per year (figure 15). Wetlands exhibit predominant hydroperiod cycles of an approximate 180 day (semi-annual) seasonality (Foster, 2007), which is equivalent to 2 cycles per year (figure 15). The frequencies detected in the dataset reflect changes observed in daily and seasonal variations in temperature and radiance. The 1 and 2 cycles per year frequencies observed in the water level data are also present in the Partoun temperature, precipitation, and reference evapotranspiration data, and are most prominent in the temperature data and least prominent in the rainfall data (figure 16). Wavelet analysis of the piezometer data demonstrated that daily periodicity was limited to summer months, supporting the idea that daily water level fluctuations are predominantly driven by evapotranspiration (figure 17). While I conducted multiple cross wavelet analyses and compared multiple variables, I found no compelling coherence signals besides the yearly seasonal periodicity apparent in most of the datasets.

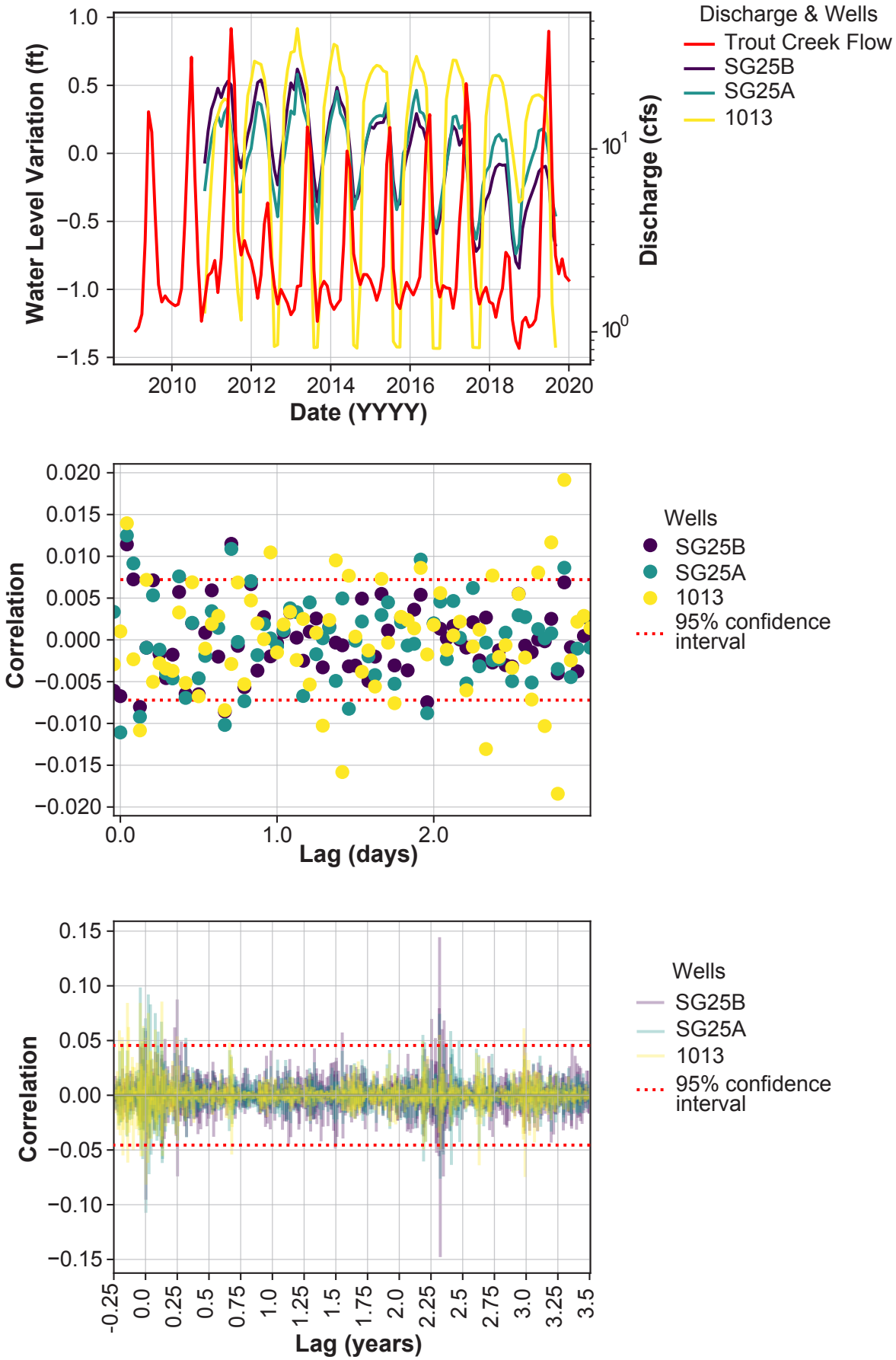

Figure 13. *Correlation between Trout Creek discharge and water levels at wells SG25A, SG25B, and 1013.*

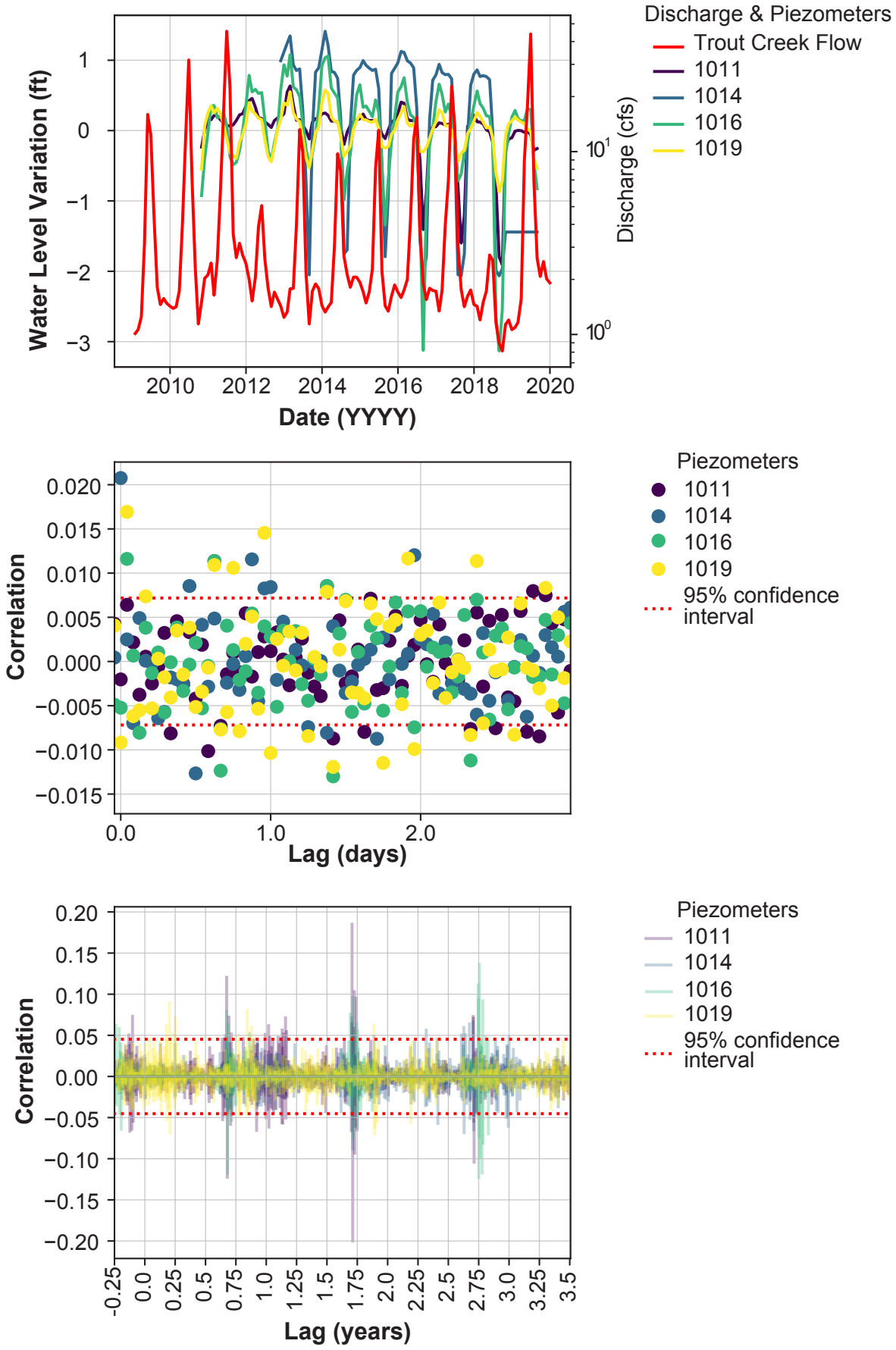

Figure 14. *Correlations between Trout Creek discharge and water levels at piezometers 1011, 1014, 1016, and 1019.*

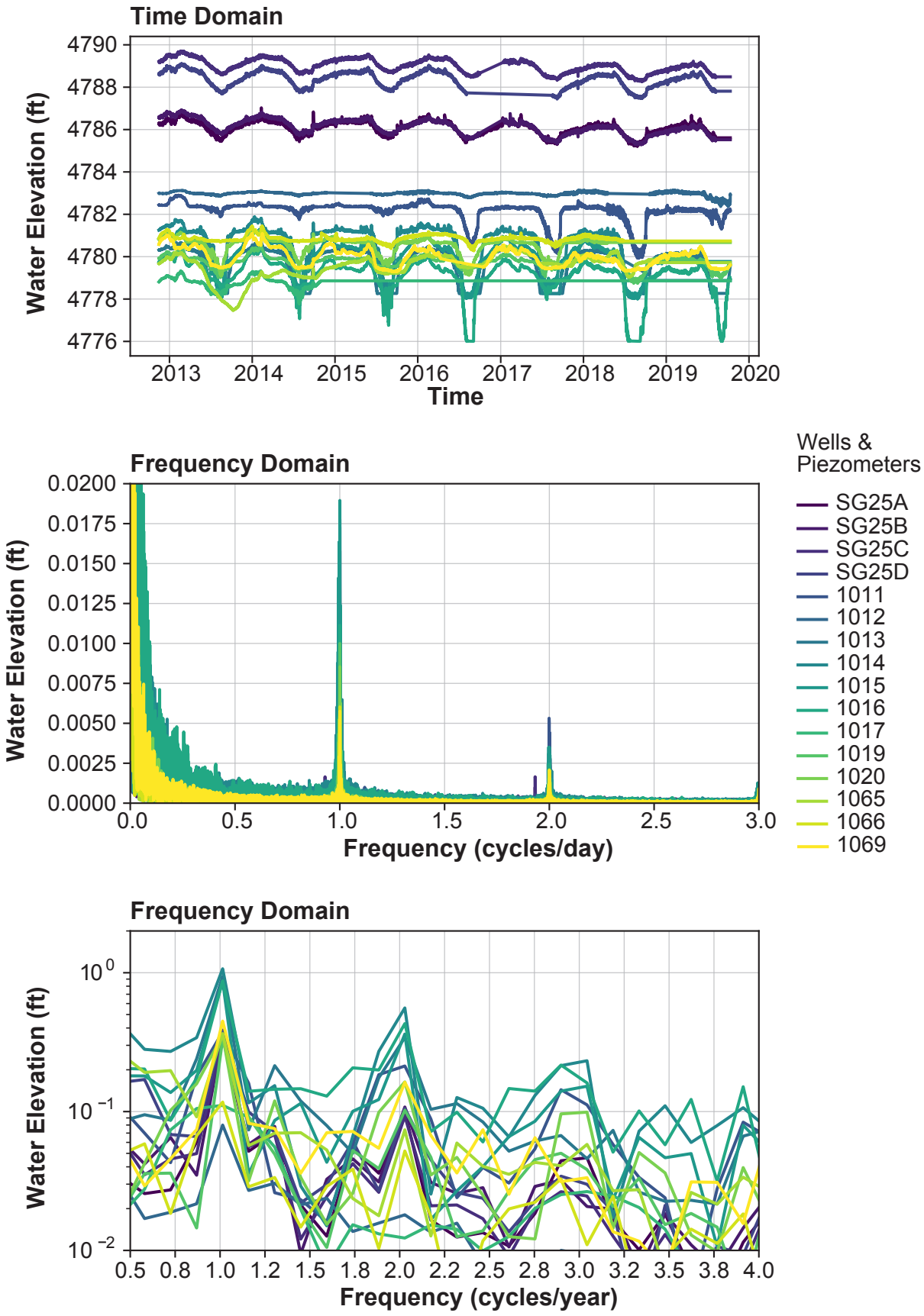

Figure 15. *Fast Fourier Transform of wells and piezometer data in Leland Harris.*

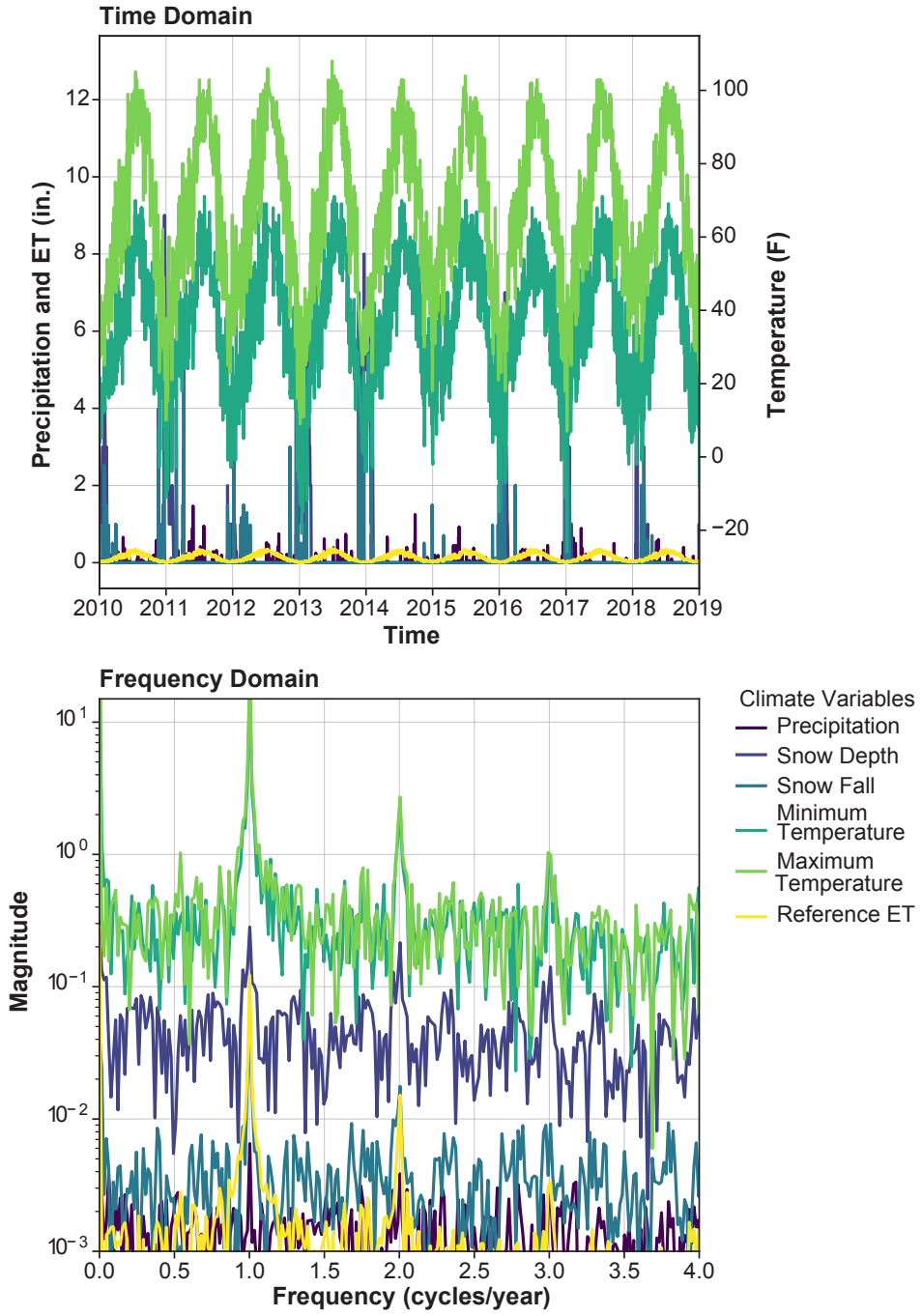

Figure 16. *Fast Fourier Transform of climate station data at Partoun.*

Elevations

The lidar data were extremely valuable for this study and the most accurate elevation dataset available for Leland Harris. I made considerable effort to assign elevations to the measurements made by Grover (2019) and connect those elevations to the groundwater elevations measured in the piezometers and spring gradient wells. Grover (2019) was successful in performing linear regressions that predicted surface water levels based on groundwater elevations, determining SG25D as an effective predictor. However, there are no elevations associated with his measurements besides those derived from the lidar data.

Based on Grover's (2016) isoline map for April to May 2013, water extended to the 1457.1 meter (4780.5 ft) contour in most parts of Leland Harris, with higher surface water elevations in the Hidden Spring and Muskrat Spring (northwest) part of the wetland system. To calculate patch parameters deemed important for species health, continuous surface water elevations would be valuable. The elevations reported at each piezometer are generally higher than the estimated surface water elevations near the piezometer, which may be caused by differences between the vertical datums of the lidar and the data from the high precision GPS surveys.

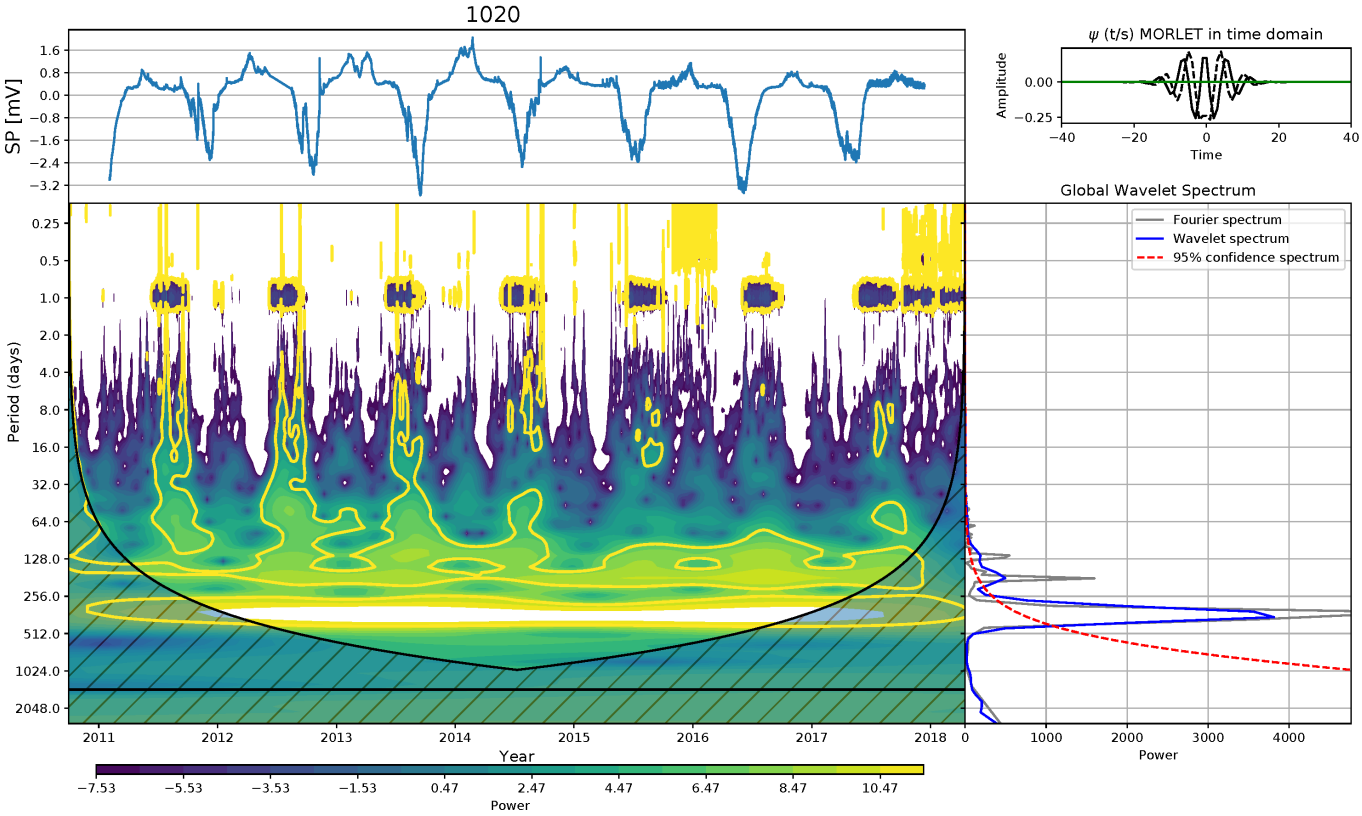

Figure 17. *Wavelet analysis of piezometer 1020 showing changes in major periodicities over time. Values highlighted in yellow indicate a significant frequency in the dataset.*

Elevation analysis of the lidar data resulted in a set of hypsometric curves, one for area and one for volume (figure 18). The hypsometric curves show an exponential relationship between water surface elevation and area covered. The trends from the lidar data match those calculated by Grover (2016) from his bathymetric measurements. The hypsometric curves are unreliable below the limitations of the lidar data (1456 m), and therefore the curves likely underestimate the total area and volume of inundation, and neglect the deeper isolated pools.

Model Results

The PASTAS model provided mixed results (table 5). Of the stressors and distributions applied in the model, ET with a Hantush distribution provided the best fits, where AIC and the root mean squared error are lowest, and the r-squared value is highest. The Hantush distribution is usually applied to models of well pumping, and the superior fit of this distribution to an ET stressor implies that the wetland plants are acting as an agglomeration of multiple tiny pumping wells as they transpire. The wells had a higher median r-squared and lower error with the model that used a combination of ET and precipitation, but the piezometers matched better to a model that relied solely on ET as the stressor. SG25B had the best fit, with an r-squared value of 84.7% when using the ET and precipitation model. Piezometers 1015, 1017, and 1019 generally had the best fits of the piezometers within all the models. The worst general fit was for piezometer 1013, likely due to the data gaps during the driest parts of the season for that well. Precipitation produced the poorest results, with very low r-squared values and relatively high errors. The model failed to correctly model the plateaus (flattening periods) of the wetland time series, especially prevalent in piezometers 1011, 1013, 1014, and 1020 (figure 19). The peaks of the modeled data in these wells rose well above the measurements. The model excellently represents the deeper spring gradient wells, which may indicate it is not entirely adequate for a complex system having a close tie between groundwater and surface water. Modeling the ET using a response function commonly used for wells produced more favorable results in the wetland piezometers, though still did not match the shouldered shape of the hydrographs. The PASTAS model shows that ET can explain at least 30% of the variance observed in the wetland piezometers, and that plants act very much like pumping wells in the shallow aquifer system. The spring gradient wells are best modeled with a combination of ET and precipitation, and the piezometer data are better modeled using just the ET data.

The Prophet model fits were excellent, even without the input of additional predictor datasets (table 6). The best results were generated using ET as a regressor, supporting the results from the PASTAS models. Adding a regressor only marginally improved model results. The lowest R value for all model results was 0.58 for piezometer 1011, and the highest R value was 0.98 for piezometer 1020. Piezometer 1020 generally had the best fit for all the Prophet models (figure 20).

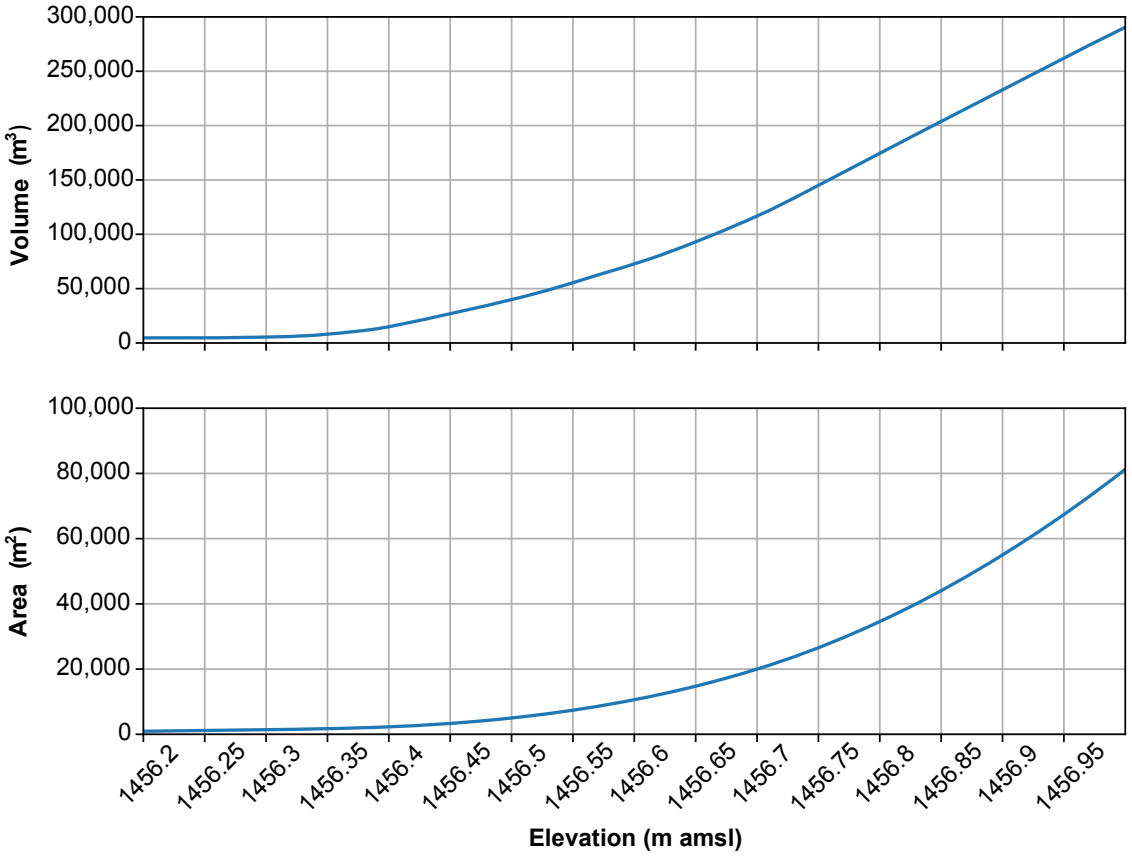

Figure 18. *Hypsometric curve of surface water in Leland Harris.*

Table 5. *Model results metrics for runs of the PASTAS model using different stressors and distributions.*

			Wells (SG25)				Piezometers											
Distribution	**Stressor**	**Measure**	**A**	**B**	**C**	**D**	**1011**	**1012**	**1013**	**1014**	**1015**	**1016**	**1017**	**1019**	**1020**	**Med. Wells**	**Med. Piez.**	**Model Rank**
Gamma	ET	RSQ (%)	69	82	51	62	28	0	0	27	70	41	74	74	63	66	41	2
		AIC	7.1	10.0	10.2	10.2	7.9	13.7	7.4	6.8	7.5	5.5	11.1	10.6	8.9	10.1	7.9	
		RMSE	0.16	0.15	0.21	0.23	0.37	0.08	0.50	0.69	0.43	0.47	0.14	0.14	0.26	0.19	0.37	
Hantush	ET	RSQ (%)	72	48	61	73	30	29	34	57	75	51	73	76	67	66	57	1
		AIC	6.8	9.5	10.1	9.7	7.9	13.7	7.4	6.7	7.3	5.5	11.1	10.6	9.0	9.6	7.9	
		RMSE	0.16	0.25	0.19	0.19	0.37	0.06	0.39	0.58	0.39	0.43	0.14	0.14	0.24	0.19	0.37	
Gamma	ET & Precip	RSQ (%)	78	85	52	68	41	0	0	40	75	47	75	77	66	73	47	4
		AIC	13.8	16.3	16.4	16.5	14.0	19.7	13.7	12.9	13.7	11.6	17.5	16.8	15.2	16.3	14.0	
		RMSE	0.14	0.14	0.21	0.21	0.34	0.08	0.48	0.61	0.39	0.45	0.14	0.14	0.24	0.18	0.34	
Hantush (ET) Gamma (Precip)	ET & Precip	RSQ (%)	77	52	62	76	31	27	12	60	77	52	75	76	67	69	60	3
		AIC	13.6	16.0	16.4	16.2	14.0	19.8	13.7	12.8	13.7	11.6	17.5	16.8	15.2	16.1	14.0	
		RMSE	0.14	0.25	0.18	0.18	0.36	0.06	0.45	0.54	0.38	0.43	0.14	0.14	0.24	0.18	0.36	
Gamma	Precip	RSQ (%)	0.0	0.0	0.0	0.0	0.0	20.7	0.0	0.0	0.0	0.0	0.0	0.0	0.0	0.0	0.0	6
		AIC	6.7	9.5	10.0	9.6	7.8	13.7	7.0	6.5	7.1	5.4	10.8	10.4	8.7	9.5	7.8	
		RMSE	0.32	0.42	0.32	0.39	0.45	0.07	0.55	2.01	0.81	0.64	0.29	0.29	0.43	0.36	0.45	
Gamma	Temp	RSQ (%)	72	43	12	66	29	33	28	48	69	52	74	76	62	55	52	5
		AIC	7.1	10.2	10.3	10.3	7.9	13.7	7.2	6.6	7.3	5.5	11.0	10.6	8.8	10.2	7.9	
		RMSE	0.16	0.27	0.28	0.21	0.37	0.06	0.41	0.67	0.44	0.43	0.14	0.14	0.26	0.24	0.37	

RMSE is the root mean squared error
RSQ is the r-squared value
AIC is the Akaike information criterion
ET is evapotranspiration

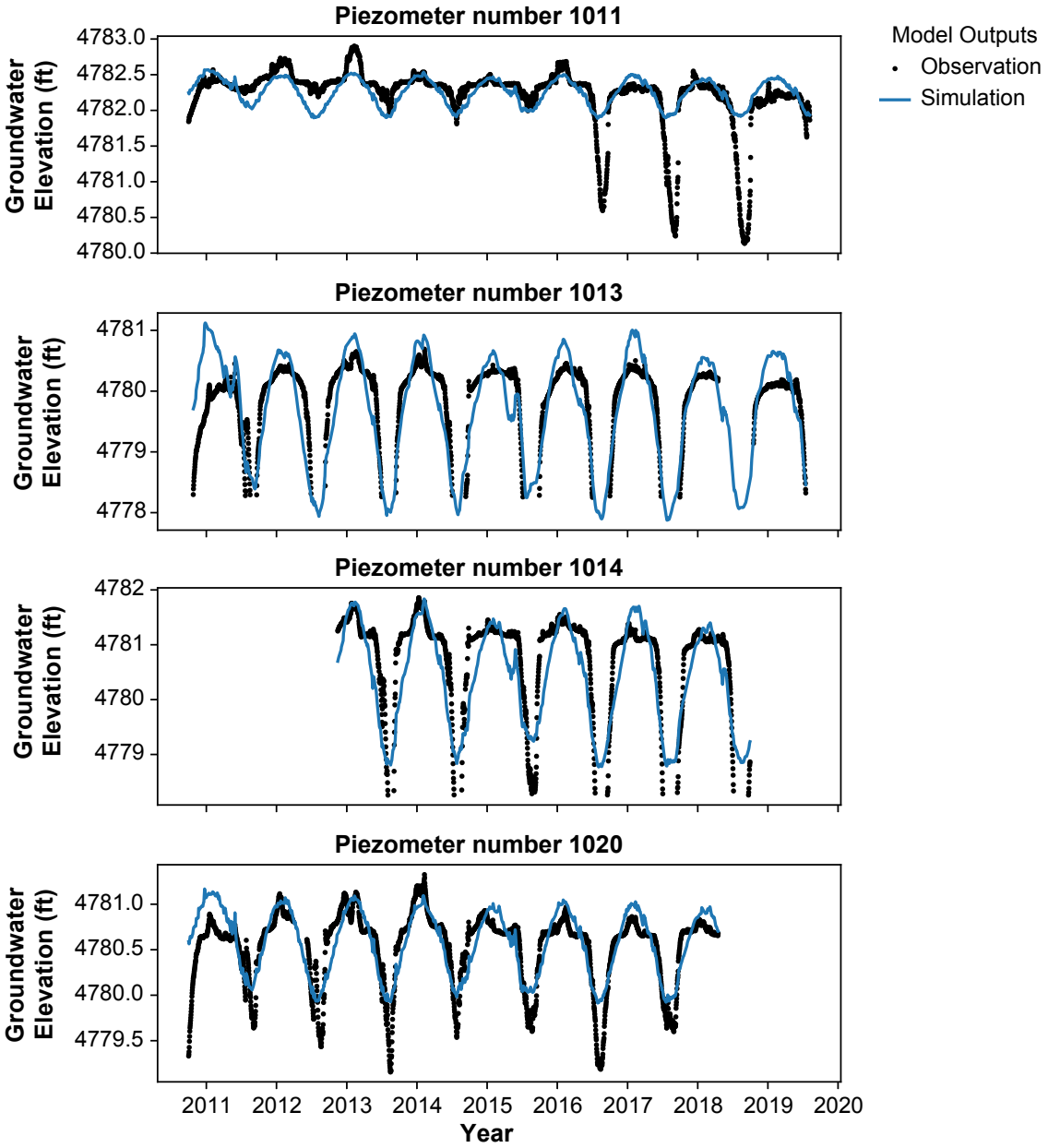

Figure 19. *Comparison of water level measurements (black dots) to PASTAS model predictions (blue lines).*

Table 6. *Fit parameters to water level data from the Prophet models.*

Predictor	Measure*	SG25A	SG25B	SG25C	SG25D	1011	1012	1013	1014	1015	1016	1019	1020
Temperature	R	0.89	0.89	0.89	0.84	0.61	0.73	0.89	0.97	0.96	0.75	0.91	0.97
Temperature	MAE	0.17	0.22	0.24	0.42	0.6	0.09	0.16	0.19	0.2	0.4	0.09	0.14
Trout Creek Flow	R	0.87	0.88	0.89	0.83	0.58	0.81	0.91	0.97	0.96	0.75	0.91	0.97
Trout Creek Flow	MAE	0.18	0.22	0.24	0.44	0.62	0.07	0.13	0.17	0.2	0.4	0.09	0.13
Evapotranspiration	R	0.89	0.89	0.89	0.84	0.58	0.75	0.89	0.97	0.96	0.76	0.91	0.98
Evapotranspiration	MAE	0.16	0.21	0.22	0.4	0.62	0.09	0.16	0.13	0.2	0.4	0.09	0.13
Precipitation	R	0.88	0.88	0.89	0.84	0.61	0.79	0.89	0.97	0.96	0.75	0.91	0.98
Precipitation	MAE	0.18	0.23	0.24	0.44	0.6	0.08	0.16	0.13	0.2	0.4	0.09	0.13
Existing Water Levels[1]	R	0.88	0.88	0.89	0.84	0.61	0.81	0.89	0.97	0.96	0.75	0.91	0.98
None	MAE	0.18	0.22	0.24	0.43	0.6	0.07	0.14	0.15	0.2	0.39	0.09	0.13

*R is the Pearson's R correlation coefficient; MAE is the mean absolute error

[1]Existing Water Levels refers to using only the previous water level measurements at the station being predicted.

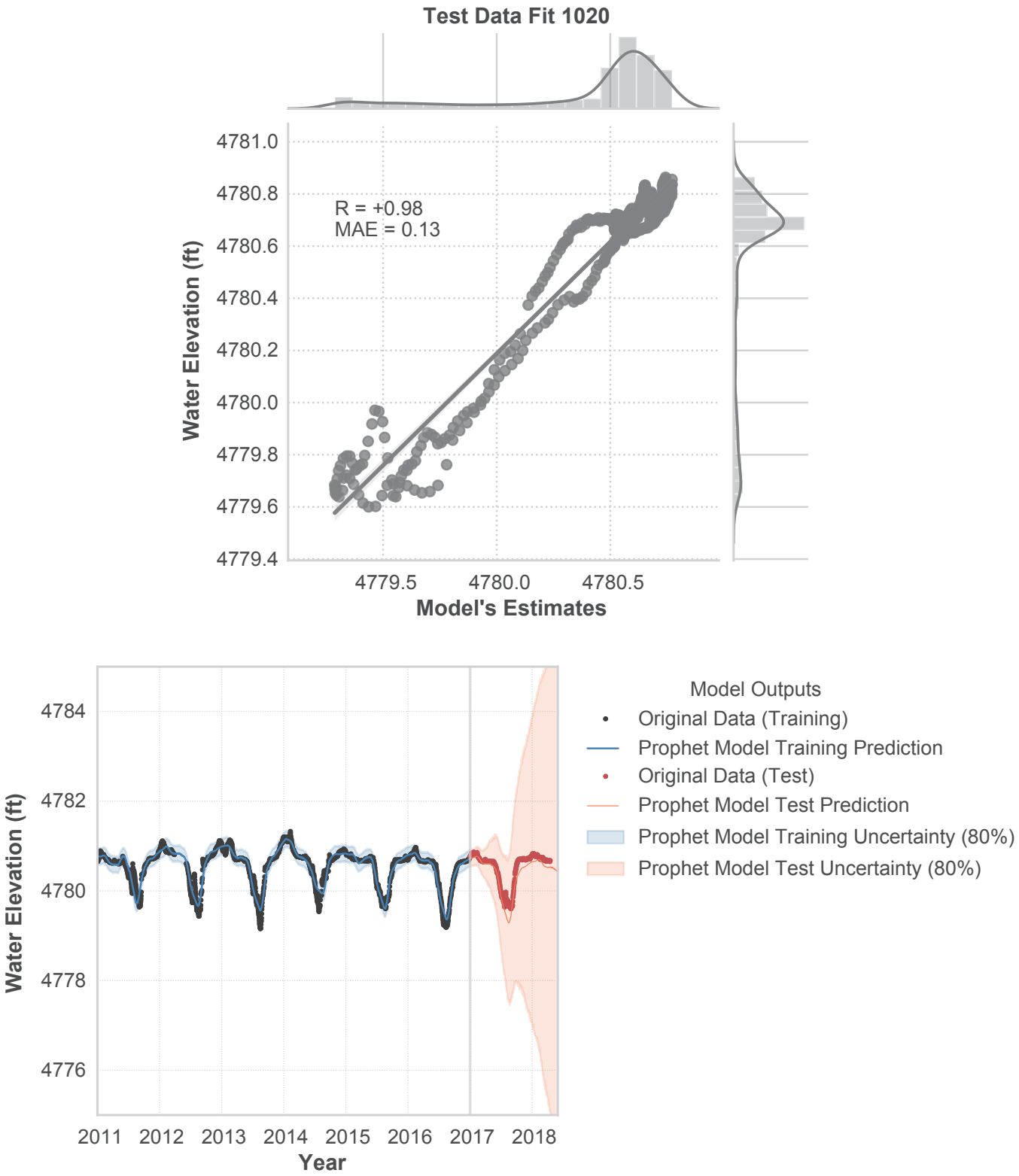

Figure 20. *Example of Prophet model output of piezometer 1020.*

CONCLUSIONS

Due to seasonal dependence, piezometer data can be modeled with minimal supplementary predictor data. Advanced time series models can predict wetland groundwater level fluctuations to a high degree of accuracy just by using the available existing data from the piezometer. In terms of predictors, the groundwater levels in the piezometers are predominantly controlled by evapotranspiration, which in turn is predominantly controlled by temperature. The best regressors for the piezometers are precipitation, evapotranspiration, and nearby stream discharge. Increasing trends in temperature will lead to increases in evapotranspiration and lowering of the groundwater level in the wetland complex. More than half of the variation observed in the seasonal trends was caused by evapotranspiration. Long-term trends appear to reflect variations in total snowpack volume, although the response data appear to have a one to three-year lag. The 10-year measurement interval was not sufficient to compare to the greater climate indices, but those indices drive snowpack.

ACKNOWLEDGMENTS

This report describes the methods and results of *Project 2, Task 1: Climate Effects on Groundwater-dependent Wetlands*, which was funded by Wetland Program Development Grant assistance ID number CD-96851101-2. I thank Mark Grover for generously sharing the data he collected. Thanks to Rich Emerson for brainstorming the key elements of this project. Thanks to Rich Emerson, Lindsey Smith, and Peter Goodwin for collecting the piezometer data. Drew Dittmer provided very valuable support on how this project could be applied to sensitive species. Diane Menuz did an amazing job managing this project, keeping me on task, contributing thoughtful approaches, and providing a technical review. Thanks to Hugh Hurlow, Stephanie Carney, Kimm Harty, Mike Hylland, and Bill Keach for their time and care in reviewing this manuscript.

REFERENCES

von Asmuth, J.R., Bierkens, M.F.P., and Maas, K., 2002, Transfer function-noise modeling in continuous time using predefined impulse response functions: Water Resources Research, v. 38, no. 12, p. 1–12, doi: 10.1029/2001WR001136.

von Asmuth, J.R., Maas, K., Bakker, M., and Petersen, J., 2007, Modeling time series of ground water head fluctuations subjected to multiple stresses: Ground Water, v. 46, no. 1, p. 30–40, doi: 10.1111/j.1745-6584.2007.00382.x.

Collenteur, R.A., Bakker, M., Caljé, R., Klop, S.A., and Schaars, F., 2019, PASTAS—Open source software for the analysis of groundwater time series: Groundwater, v. 57, no. 6, p. 877–885, doi: 10.1111/gwat.12925.

Cooper, D.J., Sanderson, J.S., Stannard, D.I., and Groeneveld, D.P., 2006, Effects of long-term water table drawdown on evapotranspiration and vegetation in an arid region phreatophyte community: Journal of Hydrology, v. 325, no. 1, p. 21–34, doi: 10.1016/j.jhydrol.2005.09.035.

Cooper, D.J., Wolf, E.C., Ronayne, M.J., and Roche, J.W., 2015, Effects of groundwater pumping on the sustainability of a mountain wetland complex, Yosemite National Park, California: Journal of Hydrology: Regional Studies, v. 3, p. 87–105, doi: 10.1016/j.ejrh.2014.10.002.

Dickey, D.A., and Fuller, W.A., 1979, Distribution of the estimators for autoregressive time series with a unit root: Journal of the American Statistical Association, v. 74, no. 366a, p. 427–431, doi: 10.1080/01621459.1979.10482531.

Fahle, M., and Dietrich, O., 2014, Estimation of evapotranspiration using diurnal groundwater level fluctuations: Comparison of different approaches with groundwater lysimeter data: Water Resources Research, v. 50, no. 1, p. 273–286.

Foster, L.D., 2007, Using frequency analysis to determine wetland hydroperiod: Tampa, Florida, University of South Florida, 120 p.

Gardner, P.M., Masbruch, M.D., Plume, R.W., and Buto, S.G., 2011, Regional potentiometric-surface map of the Great Basin carbonate and alluvial aquifer system in Snake Valley and surrounding areas, Juab, Millard, and Beaver Counties, Utah, and White Pine and Lincoln Counties, Nevada: Scientific Investigations Map 3193.

van Geera, F.C., and Zuur, A.F., 1997, An extension of Box-Jenkins transfer/noise models for spatial interpolation of groundwater head series: Journal of Hydrology, v. 192, no. 1–4, p. 65–80, doi: 10.1016/S0022-1694(96)03113-7.

Gribovszki, Z., Kalicz, P., Szilágyi, J., and Kucsara, M., 2008, Riparian zone evapotranspiration estimation from diurnal groundwater level fluctuations: Journal of Hydrology, v. 349, no. 1, p. 6–17, doi: 10.1016/j.jhydrol.2007.10.049.

Grover, M.C., 2016, Relationships of groundwater levels to surface water fluctuations and habitat associations of Least Chub (Iotichthys Phlegethontis) in a Great Basin spring complex, *in* Comer, J.B., Inkenbrandt, P.C., Krahulec, K., and Pinnell, M.L., editors, Resources and geology of Utah's west desert: Salt Lake City, Utah, Utah Geological Association Publication 45, p. 247–272.

Grover, M.C., 2019, Effects of groundwater fluctuations on the distribution and population structure of two cyprinid fishes in a desert spring complex: Journal of Freshwater Ecology, v. 34, no. 1, p. 167–187, doi: 10.1080/02705060.2019.1578699.

Hays, K.B., 2003, Water use by saltcedar (Tamarix sp.) and associated vegetation on the Canadian, Colorado and Pecos Rivers in Texas: Texas A&M University, 98 p.

Heilweil, V.M., and Brooks, L.E., 2011, Conceptual model of the Great Basin carbonate and alluvial aquifer system: U. S. Geological Survey Scientific Investigative Report 2010–5193, 191 p.

Hill, R.J., Barker, J.B., and Lewis, C.S., 2011, Crop and wetland consumptive use and open water surface evaporation for Utah: Utah State University Utah Agricultural Experiment Station Contract report for Utah Division of Water Resources and Division of Water Rights, Research Report No. 213, 138 p.

Hurlow, H., 2014, Hydrogeologic studies and groundwater monitoring in Snake Valley and adjacent hydrographic areas, west-central Utah and east-central Nevada: Utah Geological Survey Bulletin 135, 304 p. https://doi.org/10.34191/B-135.

Inkenbrandt, P.C., Doss, P.K., Pickett, T.J., and Brown, R.J., 2005, Barometric and earth-tide induced water-level changes in the Inglefield Sandstone in southwestern Indiana: Proceedings of the Indiana Academy of Science, v. 114, no. 1, p. 1–8.

Loheide, S.P., Butler, J.J., and Gorelick, S.M., 2005, Estimation of groundwater consumption by phreatophytes using diurnal water table fluctuations: A saturated-unsaturated flow assessment: Water Resources Research, v. 41, no. 7, doi: 10.1029/2005WR003942.

Maraun, D., and Kurths, J., 2004, Cross wavelet analysis: significance testing and pitfalls: Nonlinear Processes in Geophysics, v. 11, no. 4, p. 505–514, doi: 10.5194/npg-11-505-2004.

Masbruch, M.D., 2019, Numerical model simulations of potential changes in water levels and capture of natural discharge from groundwater withdrawals in Snake Valley and adjacent areas, Utah and Nevada: U.S. Geological Survey USGS Numbered Series 2019–1083, 49 p.

Masbruch, M.D., Gardner, P.M., and Brooks, L.E., 2014, Hydrology and numerical simulation of groundwater movement and heat transport in Snake Valley and surrounding areas, Juab, Miller, and Beaver Counties, Utah, and White Pine and Lincoln Counties, Nevada: US Geological Survey Scientific Investigations Report 2014–5103, 107 p., doi: 10.3133/sir20145103.

van Oldenborgh, G.J., 2020, KNMI Climate Explorer: Online, https://climexp.knmi.nl/start.cgi, accessed December 2019.

Patten, D.T., Rouse, L., and Stromberg, J.C., 2008, Isolated Spring Wetlands in the Great Basin and Mojave Deserts, USA: Potential Response of Vegetation to Groundwater Withdrawal: Environmental Management, v. 41, no. 3, p. 398–413, doi: 10.1007/s00267-007-9035-9.

PRISM Climate Group, 2019, 30-year normal precipitation data sets: Online, http://prism.oregonstate.edu/normals/, accessed March 2019.

Sáenz, J., 2014, Patch dynamics of desert fishes in the arid wetlands of western Utah: Corvallis, Oregon, Oregon State University, 130 p.

Seabold, Skipper, and Perktold, J., 2010, Statsmodels—econometric and statistical modeling with Python: Proceedings of the 9th Python in Science Conference, Proceedings of the 9th Python in Science Conference.

Taylor, S.J., and Letham, B., 2017, Forecasting at scale: PeerJ Preprints preprint, doi: 10.7287/peerj.preprints.3190v2.

U.S. Geological Survey, 2019, National Water Information System (NWIS)—water data for the nation: Online, https://waterdata.usgs.gov/nwis, accessed May 2019.

White, W.N., 1932, A method of estimating ground-water supplies based on discharge by plants and evaporation from soil: Results of investigations in Escalante Valley, Utah: U.S. Government Printing Office USGS Numbered Series 659-A, 115 p.

Zotarelli, L., Dukes, M.D., Romero, C.C., Migliaccio, K.W., and Morgan, K.T., 2010, Step by Step Calculation of the Penman-Monteith Evapotranspiration (FAO-56 Method): Agricultural and Biological Engineering Department Extension Report AE459, 10 p.